Durham E-Theses

Synthesis and Photophysics of Cyclometalated Ir(III) Complexes with Novel 4-Substituted-2-Phenyl-Pyridine Ligands

LI, CHENFEI

How to cite:

Use policy

Abstract

This thesis reports the design, synthesis and photophysical characterisation of a series of novel cyclometalated iridium complexes with 4-substituted-2-phenyl-pyridine ligands. A synthetic strategy based on preparation of 4-substituted pyridine and subsequent phenylation was applied, and related challenges, for instance, the preparation of 4-(4'(-iodo-2',3',5',6'-tetramethylphenyl)pyridine from 1,4-diiododurene, low yields of the Sonogashira reactions due to the steric hindrance and low yields of phenylation reactions with phenyl lithium have been overcome. Photophysical studies show that the π-conjugation of iridium complexes broken by rotating the 4-substituents out of plane, and this kind of complexes exhibit similar emission spectra to the unsubstituted parent compound Ir(ppy)$_2$(acac). **C4** shows an extremely long luminescence lifetime for a complex of this type, and the nature of this characteristic may be due to the triplet energy being distributed between the ligand and the metal centre.

Key words: iridium complex, phosphorescence, green emission, functionalization of 2-phenyl-pyridine ligand

Acknowledgements

First and foremost, I would like to thank Professor Andrew Beeby for his support, advice and enthusiasm throughout the year.

Secondly, massive thanks should go to Dr Ross Davidson for his guidance and supervision in synthetic lab. Meanwhile, I would like to say a sincere thanks to Dr Helen Hsu for her guidance and supervision in the photophysics lab, also for her teaching and demonstrating of photophysical measurements.

Thirdly, special thanks must go to Dr Matthew Aldred for advice and good sense of humour.

Thanks must go to Stacey Lindsay, Chandni Bhagani, Thomas Batchelor and Daniel Hernandez for making the year so enjoyable and their endless advice and help.

Thank you to all the analytical staff, for the help and work to process some of the data.

Last but not least, I would like to thank my family and all my friends for their support.

Abbreviation

acac	acetylacetonate
AgOTf	trifluoromethanesulfonate
ASAP	atmospheric solids analysis probe
C^N	generic phenylpyridine type cylometalating ligand
DCM	dichloromethane
DFT	density functional theory
Dppy	2,4-diphenylpyridine
EQE	external quantum efficiency
ESI+	electrospray ionisation (positive ion)
fac	facial
Fppy	(4-formylphenyl)pyridine
GC-MS	gas chromatography- mass spectrometry
Hacac	acetylacetone
HOMO	highest occupied molecular orbital
HPLC	high purity liquid chromatography
IC	internal conversion
ISC	intersystem crossing
LC	ligand centre
LUMO	lowest unoccupied molecular orbital
MALDI-ToF	matrix assisted laser desorption/ionization-time-of-flight
MLCT	metal to ligand charge transfer
MO	molecular orbital
MS	mass spectrometry
NMR	nuclear magnetic resonance
OLED	organic light-emitting diode

PLQY	photoluminescence quantum yield
Hppy	2-phenylpyridine
R	generic organic group (unless specified)
r.t.	room temperature
SOC	spin-orbit coupling
THF	tetrahydrofuran
TLC	thin layer chromatography
TMS	trimethylsilyl
TIPS	triisopropylsilyl
UV-vis	ultraviolet-visible
VR	vibrational relaxation
XY	generic ancillary ligand

Symbols and non-SI units

A	absorbance
Å	Angstrom, $1\text{Å} = 10^{-10}\text{m}$
a.u.	arbitrary units
J	J-coupling constant for ^{1}H-NMR, Hz
M	molar concentration, $1\text{M} = 1\text{mol} \cdot dm^{-3}$
M^+	molecular ion peak in MS
m/z	mass to charge ratio in MS
ppm	parts per million
S_n	n^{th} singlet state (n=0 ground state)
T_n	n^{th} triplet state
δ	chemical shift in NMR spectroscopy, in ppm
λ_{abs}	wavelength of absorption, nm
λ_{em}	wavelength of emission, nm
τ_p	phosphorescent lifetime, µs
τ_0	pure radiative lifetime, calculated by $\frac{\tau_p}{\Phi_p}$, µs
Φ_p	quantum yield of phosphorescence

List of Figures

List of Tables

List of Schemes

Table of Contents

Chapter 1 Introduction

1.0 Introduction

Recently, organic light emitting diodes (OLEDs) have become a 'hot topic' of research for both academia and industry, due to a great range of potential advantages over the current frontrunners: inorganic light emitting diodes (LEDs) and liquid crystal displays (LCDs). They are thinner, lighter, and potentially flexible and have lower energy consumption, making them ideally suited for display technologies but also solid-state lighting.[1, 2]

One of the most studied fields for OLED advancement is the development of the emissive layer, with the aims of increasing the stability, colour purity, and efficiency of a device while still being able to produce a range of different colours. There are two classes of emissive materials that can be employed for use in an OLED based on their mechanism of emission; i) fluorescence[3] and ii) phosphorescence[4]. Fluorescent materials containing molecular and polymeric materials, typically comprising derivatives of PPV,[5] carbazole,[6] fluorene[7] and coumarin.[8] OLED displays show many advantages over current TFT-LCD displays. However, devices based upon fluorescent materials are only able to harvest the singlet excitons generated by charge transport, giving them a maximum theoretical efficiency of 25%.[9] Phosphorescent materials, however, are able to employ both singlet and triplet excitons, giving them a theoretical maximum efficiency of 100 %.[9]

Because of their strong spin-orbit coupling (SOC), cyclometalated heavy metal complexes, especially platinum group metal complexes, are able to relax the spin-forbidden nature of the radiative decay pathway from the triplet state.[10] Given this property, cyclometalated complexes are considered to offer the greatest potential as phosphorescent emitters for OLEDs. Of these, cyclometalated iridium(III) complexes show the greatest promise due to their high photoluminescence quantum yields (PLQY), short phosphorescence lifetimes (usually 1-5 μs), and tuneable emission colour.[11, 12]

The first iridium complex studied in detail was the homoleptic cyclometalated iridium complex, fac-Ir(ppy)$_3$, where ppy is the cyclometalating 2-phenylpyridine.[13, 14] After that, more complexes based on substituted ppy ligands including new homo-leptic iridium(III) complexes, $e.g.$ Ir(fppy)$_3$,[15, 16] and heteroleptic complexes, $e.g.$ Ir(ppy)$_2$(acac),[17] were synthesised. Since then, a wide range of modified ligands have been prepared as a means of developing a simple pathway to tune the emission spectrum (many good examples of red, green and blue emitting materials have now been produced) and many with high PLQY, with several examples reaching almost 100%.[16, 18, 19]

1.1 OLEDs-mechanism, structure, characterization and materials

An organic light emitting diode, is device which exploits the electroluminescence of some special organic materials, and as a result emits light directly from an electrical

current. Electroluminescence arises from the recombination of electrons and holes carried by molecules in the form of radical ions to generate excited electronic states (excitons).[20, 21] **Figure 1** shows the simplified mechanism of an OLED device, electrons and holes are injected from the cathode (*e.g.* calcium) and the anode (*e.g.* indium tin oxide (ITO) respectively) towards the active layer. Within this layer there is charge recombination giving rise to the formation of excited states from which photons are emitted.[22]
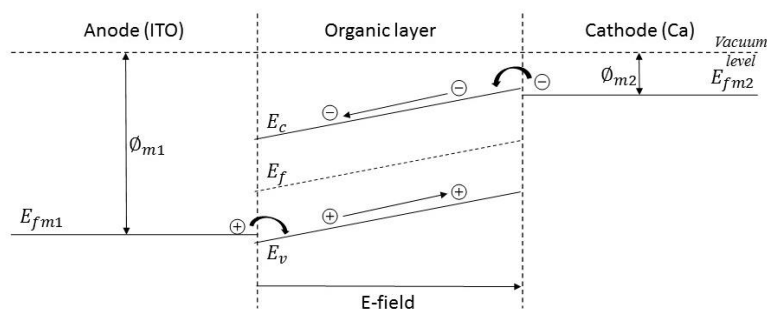
Figure 1 *OLEDs structure and mechanism adapted from reference*[23]

Therefore, an OLED device contains at least three components, anode, cathode and organic layer. Much more complicated device structures have been designed and fabricated with the purpose of enhancing output efficiency, *e.g.* a double-layer OLED device is made by anode-hole transport layer-*n*-type emitter layer-cathode;[21] a triple-layer OLED device could be made by either anode-hole transport layer-emitter layer-

electron transport layer-cathode or anode-*p*-type emitter layer-current limiting layer-*n*-type emitter layer-cathode.[24]   With the introduction of hole/ electron blocking or electrode modifying layers, OLEDs with even more complicated structures could be made in order to further increase the output efficiency.[25, 26]

There are two main measurements used to determine the usefulness of an OLED, its emission spectrum and energy conversion efficiency. The luminous power efficiency (L_{eff}) [lm $\cdot$ W^{-1}] [27] is defined as **Formula 1**.

$$L_{eff} = \frac{\pi L}{JV}$$

Formula 1: *Definition of luminous power efficiency (*L$_{eff}$*) [*lm $\cdot$ W^{-1}*]*

Where L is the luminance [cd $\cdot$ m^{-2}], while J and V are the current density [A $\cdot$ m^{-2}] and applied voltage [V] needed to obtain the luminance respectively. Another significant factor is external quantum efficiency (Φ_{ext}),[27] which is defined as the number of photons emitted per number of injected charge carriers and is expressed as **Formula 2**.

$$\emptyset_{ext} = \frac{\pi L \int \frac{F'(\lambda)\lambda}{hc} d\lambda}{\int F'(\lambda) K_m y(\lambda) d\lambda} \cdot \frac{e}{J}$$

Formula 2: *Definition of external quantum efficiency (*Φ_{ext}*), where L, c, λ, J, h and e represent pathlength, velocity of light, wavelength, current density, Planck constant and electric charge respectively*

These two different indexes are however determined by same factors: efficiency of charge carrier injection from the anode and the cathode at low drive voltage, charge balance, spin multiplicity of the luminescent state, photoluminescence (PL) quantum yield, and extraction of the emission out of the device.[27] Therefore, one way in which the efficiency of a device can be improved is to increase the photoluminescence quantum yield of the emitting species. [28]

Red, green and blue are the three primary colours, and the basis of colour display screen technology under the RGB colour model. All visible luminous colours can be generated by different combination of them. Thus, emitters are usually categorised according to their colour of emission, while they are also often discussed according to whether they are fluorescence or phosphorescent materials (see **Figure 2**).
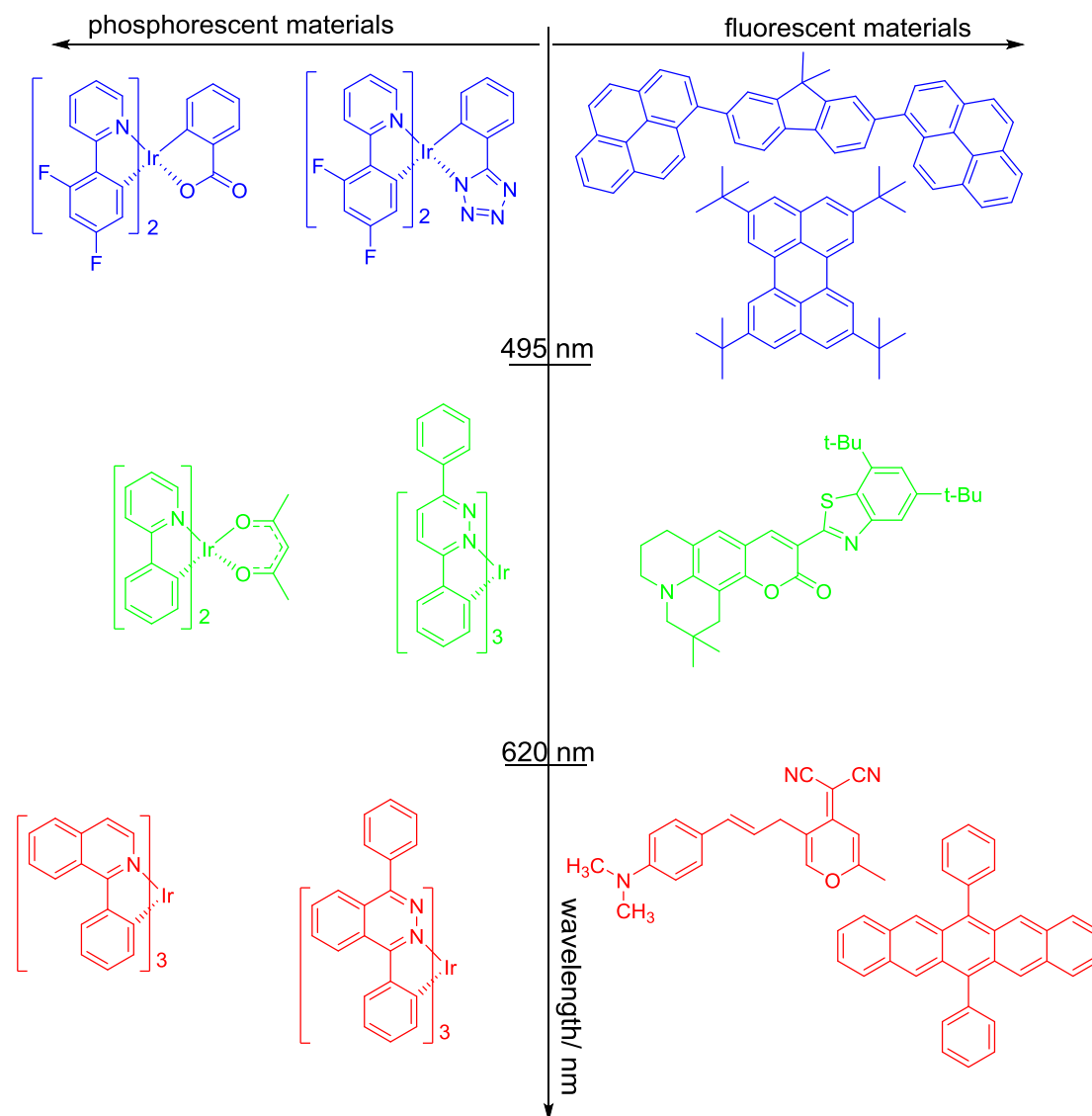
Figure 2 *Examples of blue, green and red emitting molecular materials according to the mechanism of the emission, phosphorescent materials[29-34] and fluorescent materials[35-39]*

1.2 Cyclometalated iridium complexes -synthesis and photophysics

As mentioned previously, cyclometalated iridium complexes have attracted intense interest from many scientific researchers, due to their feature of high phosphorescence quantum yield, OLEDs could also benefit from this class of materials due to the large Stokes shift by inhibit the re-absorbance of emitted light.[40]

The general structure of cyclometalated iridium(III) complexes consist of a mononuclear iridium centre surrounded by three bidentate ligands bonded by C and N atoms (C^N) to give the homoleptic complexes or with two C^N ligands and either a single bidentate ancillary ligand or two monodentate ligands giving an octahedral coordination environment.[41] Two of the most commonly used bidentate ancillary ligands are acetylacetonate (acac) and picolinate (pic), but there are numerous others have been reported.

The standard synthesis of a cyclometalated iridium complex, whether using conventional or microwave heating, involves a two-step process (see **Scheme 1**): i) the C^N ligand is reacted with $IrCl_3$ xH_2O to give a chloro-bridged Ir(III) dimer[42]; and then ii) the chloro-bridged Ir(III) dimer is treated with the ancillary ligand. Depending on the choice of ligand it may be necessary to add a base to form an anionic ligand or a halide abstractor such as AgOTf to make the dimer more reactive. This modular synthesis makes these complexes easy to prepare.

$$2IrCl_3 \cdot xH_2O + 4(C\wedge N) \xrightarrow[\text{2-ethoxyethanol}]{H_2O,} \quad \xrightarrow[\substack{K_2CO_3, \\ \text{ancillary ligand(XY)}}]{(C\wedge N) \text{ or}} \quad \substack{Ir(C\wedge N)_3 \\ \text{or} \\ Ir(C\wedge N)_2(XY)}$$
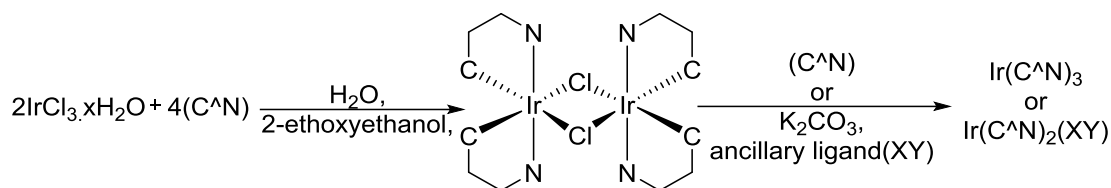
Scheme 1 *General synthesis of homo- and hetero-leptic iridium(III) complexes*

1.2.1 Ligand synthesis

With the purpose of enhancing luminescence efficiency or tuning colour, more and more novel cyclometalating ligands have been synthesised.[29-34] Phenyl pyridine based ligands have proved to be some of the most popular due to their ease of modification particularly on the phenyl ring. Cyclising and coupling, such as Suzuki-Miyaura reaction, Stille reaction and Negishi reaction, are the most extensive used techniques when synthesising substituted Hppy. In this section, a brief introduction of those important reactions are given.

The Suzuki-Miyaura coupling is a versatile palladium catalysed carbon-carbon forming reaction between two aromatic rings. This reaction occurs between an aromatic boronic acid or boronlan ester and an aromatic halide or pseudo halide in the presence of a base and palladium(0) catalyst, to give yield the aromatic groups joined by a single C-C bond. With extensive range of aromatic boronic acids, and halo-substituted pyridines commercially available, a range of substituted Hppy ligands have been produced using this reaction. The Suzuki-Miyaura reactions has many advantages, such as broad range of solvent choices, insensitivity to water, high yield

(usually beyond 40%), and simple purification of product in the most cases. However, it does have some disadvantages such as sensitivity to steric hindrance and that the palladium(0) catalyst is very sensitive to oxygen and is expensive. Generally, the Suzuki reaction is a reliable choice in terms of academic study.[43] Due to its importance, the catalytic cycle is presented and discussed of more details in a separate section below.
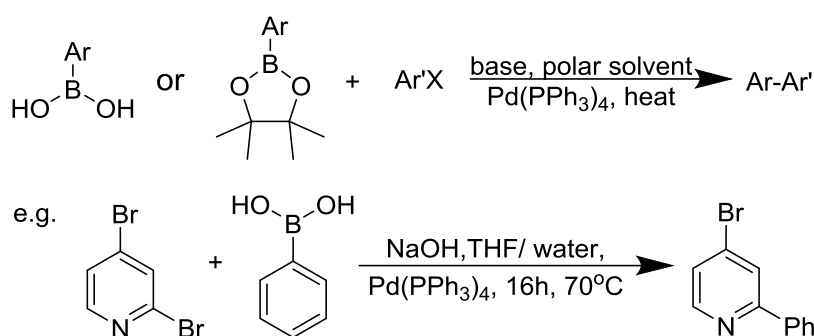
Scheme 2 *General Suzuki-Miyaura reaction with an example of making 2-phenyl-4-bromo-pyridine*

The Stille coupling is similar to the Suzuki reaction, but this reaction is performed with a stannanes replaces a boronic acid or ester, with very few limitations on the R-groups (aromatics). Well-elaborated methods allow the preparation of different products from all of the combinations of halides and stannanes depicted below. The main drawback is the toxicity of the tin compounds used, and their low polarity, which makes them poorly soluble in water. However, because it suffers from the reduced yields and slow rates of reaction for sterically hindered compounds which is

often occurs in the Suzuki reaction, the Stille coupling is still a very important route to make substituted aromatics.[44]
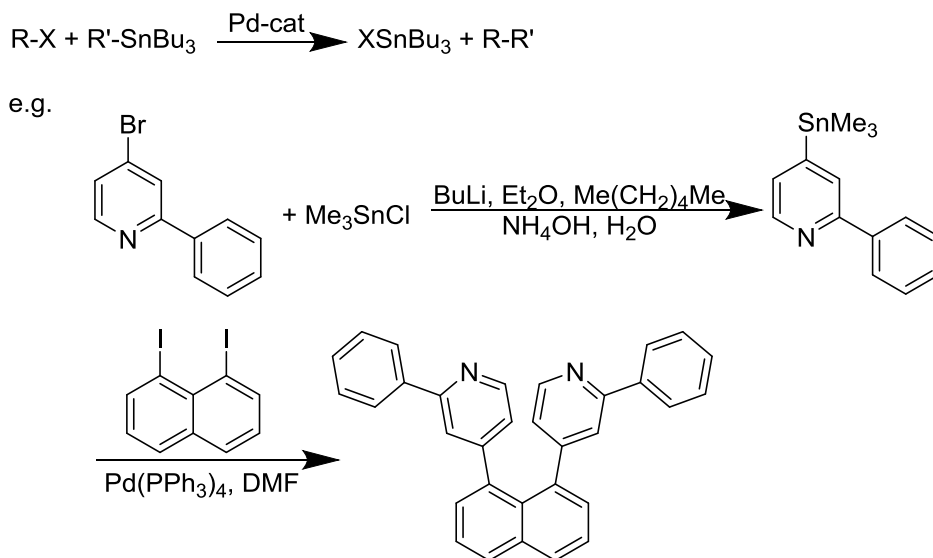
Scheme 3 *General Stille coupling and an example of making 4-substitued-bipy[45]*

The Negishi Coupling, published in 1977, was the first reaction that allowed the preparation of unsymmetrical biaryls in good yields. The versatile nickel- or palladium-catalysed coupling of organozinc compounds with various halides (aryl, vinyl, benzyl, or allyl) has broad scope, and is not restricted to the formation of biaryls.[46, 47]
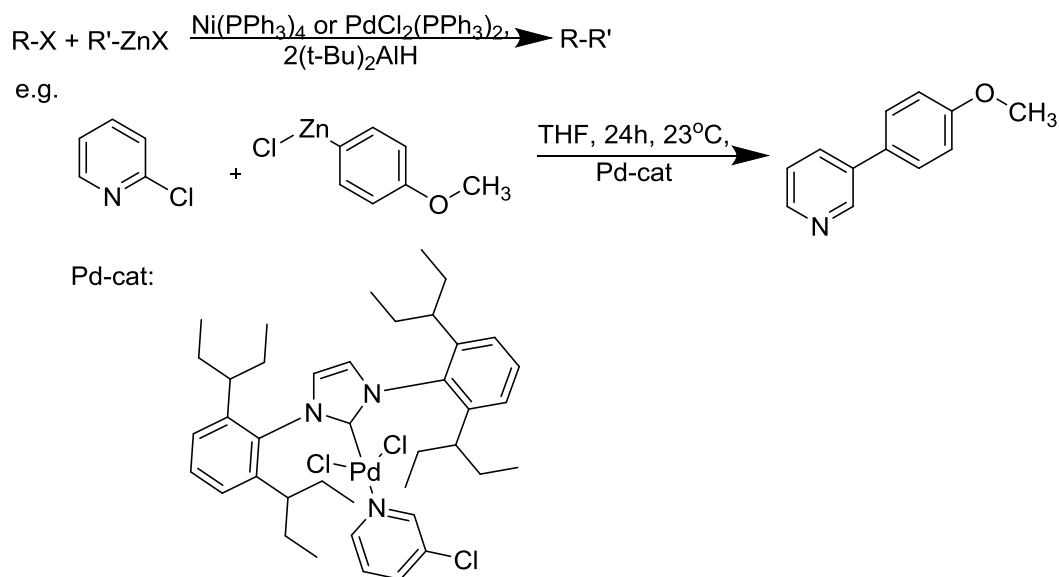
Scheme 4 *Negishi coupling with its example of making substituted-2-phenylpyridine[48]*

The Sonogashira coupling allows the coupling alkynes with aryl or vinyl halides catalysed by a palladium(0) catalyst, a copper(I) co-catalyst, and an amine base under anaerobic conditions. The Sonogashira reaction is commonly used for attaching alkynes to aromatic rings allowing the extension of linear π-conjugation and giving structural diversity. Due to its significant use within this project, catalytic cycle is presented and discussed of more details in a separate section below.
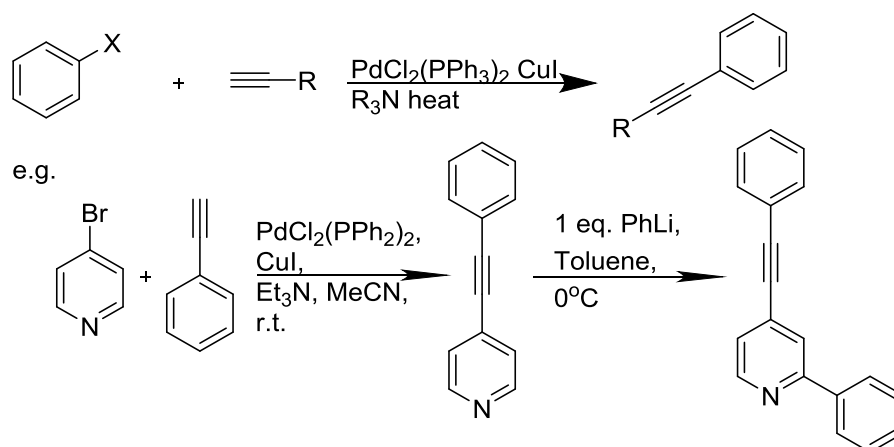
Scheme 5 General *Sonogashira reaction, and an example showing the synthesis of 4-(phenylethynyl)pyridine with subsequent phenylation of the pyridine with PhLi[49]*

The Kröhnke synthesis is a route for the synthesis of substituted pyridines, including ppy. This reaction condenses a cinnamaldehyde with a α-pyrdinium methyl ketone with a source of ammonia, and provides one the most reliable means of cyclisation to form a substituted pyridine. It has the benefit of avoiding the use of expensive catalysts. However, it is limited by the availability of the substituted cinnamaldehyde required for the synthesis. [50]
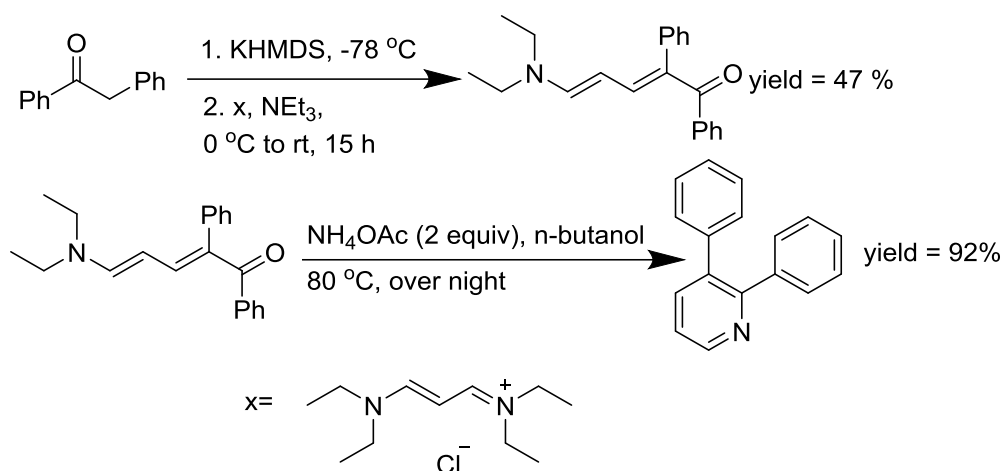
Scheme 6 *Example of a Kröhnke synthesis[51]*

1.2.2 Photophysics

A photophysical study of a cyclometalated iridium complex aims to deduce its optical properties, includes not only the emission spectrum the luminescence lifetime and quantum yields of a material, but also able to uncover the processes by which excited electronic states luminescence and relaxation pathways for a molecule,[52] and thus, indicates pathways towards higher efficiency[53] or novel applications.[54, 55] This chapter introduces the events involving excited singlet and triplet states of a cyclometalated iridium complex, and effect of substitution on the properties of 2-phenylpyridine.

As shown in the simplified *Jabłoński* diagram **Figure 3**, the possible processes in the excited states include absorption ($S_1 \leftarrow S_0$), non-radiative decay ($S_0 \leftarrow S_1$), radiative decay fluorescence ($S_0 \leftarrow S_1$) and phosphorescence ($S_0 \leftarrow T_1$) and non-radiative intersystem crossing ($T_1 \leftarrow S_1$).[56]
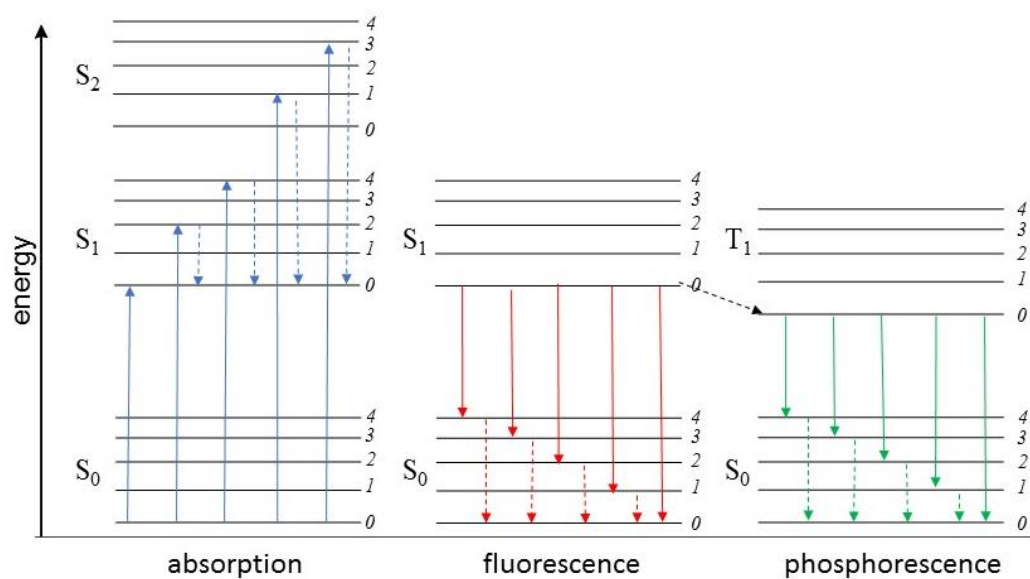
Figure 3 *Jablonski diagram representing energy levels and spectra for*

photoluminescence. Solid arrows indicate radiative transitions as occurring by

absorption (blue) or emission (red for fluorescence; green for phosphorescence) of a

photon. Dashed arrows represent non-radiative transitions (blue, green, red).

Internal conversion is a non-radiative transition, which occurs when a vibrational

state of a higher electronic state is coupled to a vibrational state of a lower electronic

state. The black dashed arrow from S(1,0)→T(1,0) is a non-radiative transition called

intersystem crossing, because it is a transition between states of different spin

multiplicity. Reproduced from common simplified Jablonski diagram

As shown in **Figure 3**, in the ground electronic state referred to as S_0 the highest lying electrons occupy the highest occupied molecular orbital, HOMO. The absorption of light can give rise to an excited singlet state which has higher energy with the formation of a hole in the HOMO and an electron in the LUMO which sometimes referred to as an exciton.[57] Excitons, depending on their different excitation source, are usually referred to as photo-generated excitons and electro-generated excitons. In terms of electro-generated excitons, when taking the spin-statistics into consideration, there are four possible spin states for exciton generated by a non-geminate pair combination due to the combination of the two half-integer spins of the two charge carriers (electrons and holes). Of these, three give a resultant spin of one *i.e.* a triplet state and only one gives the zero spin singlet state. If the recombination of the electrons and holes is statistically controlled, then only 25% of the injected charge lead to the generation of pure singlet states and 75% go to pure triplet states. Absorption could also lead to higher energy excited states *i.e.* S_2 state. Not every exciton would relax to the ground state with the emission of photons, some of them also relax via a non-radiative process. Non-radiative decay is the generic term of the following events collisional quenching, conformational change, vibrational relaxation and energy/ electron transfer. The spin-selection rule, $\Delta S = 0$, means that triplet excitons are not allowed relax back to the ground state with the emission of light. However, with the introduction of a heavy metal spin-orbit coupling contributes to strong intersystem crossing ($S_1 \rightarrow T_1$) and spin forbidden phosphorescence ($T_1 \rightarrow S_0$)

became partly allowed. Based on this, a series of phosphorescent materials are now available and, as a result, 100% internal quantum yield (IQE) finally became possible.

Homo- and heteroleptic cyclometalated iridium complexes are representative phosphorescent materials that show high photoluminescence quantum yields (more than 40%) and great potential of tuning colour.[58] One the most effective ways to modify these complexes is to add substituents to the ppy (2-phenylpyridine) ligand.[59, 60] Considering the energy levels of the frontier molecular orbits, the rule of colour tuning can be empirically explained with changes in the energies of the highest occupied molecular orbit (HOMO) and the lowest unoccupied molecular orbit with substituents. As we know, in terms of iridium ppy complexes, the phenyl moiety makes more contribution to the HOMO, while the pyridyl moiety contributes more to the LUMO. Thus, electron-withdrawing group can decrease the energy level of both HOMO and LUMO while electron-donating group can increase the energy level of HOMO and LUMO. Generally, the emission wavelength of an Ir(III)ppy$_3$ complex is blue-shifted when an electron-withdrawing group is introduced to the phenyl moiety of the phenylpyridine, while the addition of electron withdrawing groups at the pyridine causes the emission to be red-shifted.[15]

The addition of groups that extend the π-conjugation of the phenylpyridine, for example aryl or alkynyl substituents, on either the pyridine or phenyl ring leads to a red-shift in the emission. This is because as the π-conjugation is extended the

molecular orbitals become more delocalised with the result in a decrease in the band gap.[61]

substitution \ substituted position	pyridyl ring	phenyl ring
electron-donating group	blue-shift	red-shift
electron-withdrawing group	red-shift	blue-shift
extension of π-conjugation	red-shift	red-shift

Table 1 *Influence of electron-donating and withdrawing substitution on ppy ligand*

Based on this simplistic theory, the emission colour of ppy-based cyclometalated iridium complexes become tunable, and many examples of efficient emitters based upon iridium complexes containing substituted-ppy showing red, green and blue emission have been made using this approach.
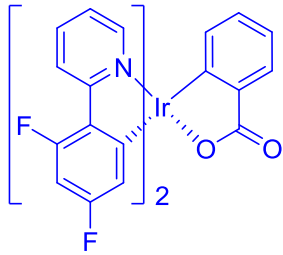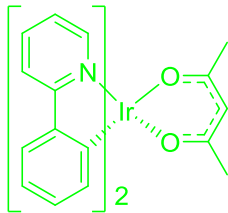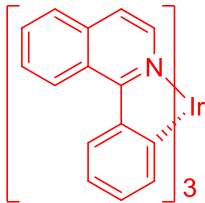
Compound	λ_{EM}/nm (emission colour)	Φ_{PL} in solution, degassed	$\tau/\mu s$ degassed
	475 (blue)	0.79	0.5
	516 (green)	0.34	1.6
	620 (red)	0.26	1.12

Table 2 *Typical examples of cyclometalated iridium emitters showing blue[16], green[31] and red[62] along with their photoluminescence properties*

1.3 Literature examples of iridium complexes with 4-substituted ppy

Before presenting more specific discussion on substituted ppy ligands and means to produce ideal emissive materials, two relevant examples will be introduced.[18, 49]

As we know, the visible spectrum is continuous, with no clear boundaries between one colour and the next. However, the typical, or commonly accepted, primary colours are required to make a colour display red (620-750 nm), green (495-570nm) and blue (450-495nm).[63] *fac*-Ir(ppy)$_3$ is a green emitter with a maximum emission wavelength of 520 nm.[64] Its heteroleptic derivate, Ir(ppy)$_2$(acac) has a similar emission spectrum.[31] In the following two examples, one is a blue-shifted complex induced by the addition of fluorine to the phenyl rings, while the other one is red-shifted by attaching an extended ethynyl-phenyl chain at the 4-position of the pyridine ring of the ligand.
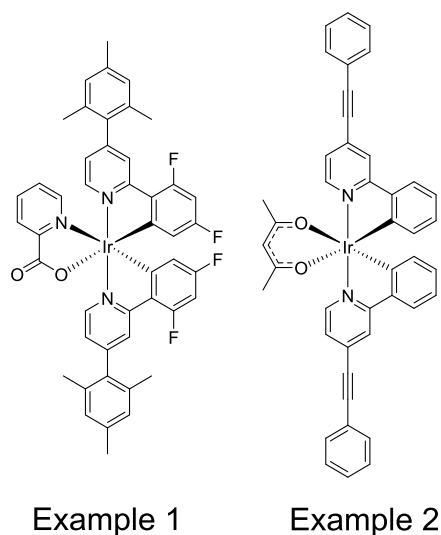
Example 1   Example 2

Scheme 7 *Two literature example of substituted-ppy*[18, 49]

complex	Φ_{PL}	λ_{em}/ nm
Example 1	0.92	473
Example 2	0.28	610

Table 3 *Photophysical properties of **examples 1 and 2***

Although **examples 1** and **2** have different design concepts and ancillary ligands, they have one obvious similarity in that both are substituted at the 4-positions of the pyridine ring. In example 1 the addition of the two fluorine atoms to each of the phenyl groups gives rise to a blue shift relative to Ir(ppy)$_2$acac, and the addition of the mesityl group at the 4-position of the pyridine ring does not give rise to any discernible red shift that might be expected due to extension of the π –system. This is because the two *o-* methyl groups of the mesityl ring force a significant torsional angle in the mesity-pyridine bond, effectively breaking the conjugation. Conversely the addition of the phenylethynyl group in example 2 does allow the extension of the π-conjugation in the ligand and a significant red shift is observed relative to Ir(ppy)$_2$acac.

In both examples, the nitrogen atoms of the pyridines are *trans* to one another (as shown in the **scheme 8**). As substituents are placed on the 4-postions of the two pyridine rings this has the effect of making the complex more prolate compared to the almost spherical parent. If this effect is desired for material property purposes then

example 1 shows that extension at these positions will not lead to a red shift if the 4-

substituent can be forced to lie at or close to 90 ° to the pyridine ring.
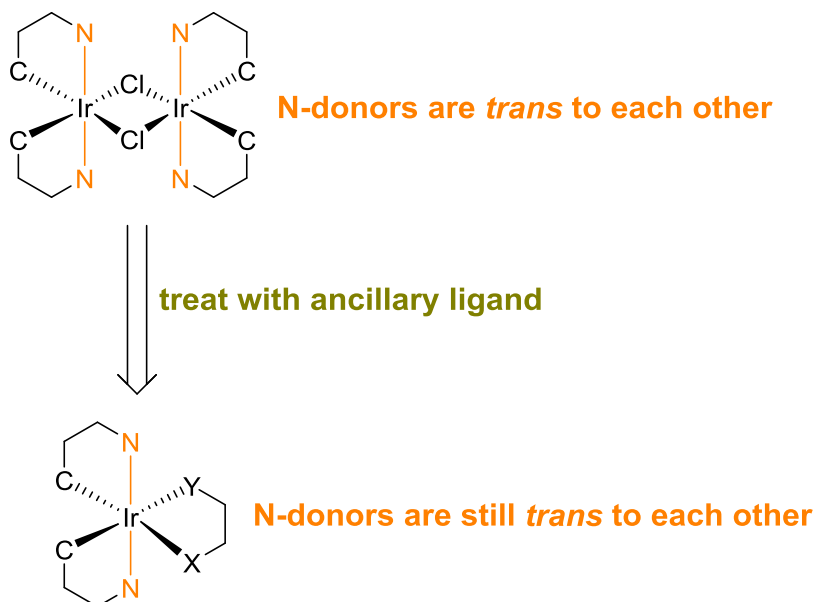
Scheme 8 *Special trans formation of N-donors in iridium dimer and Ir(C^N)2(acac)*
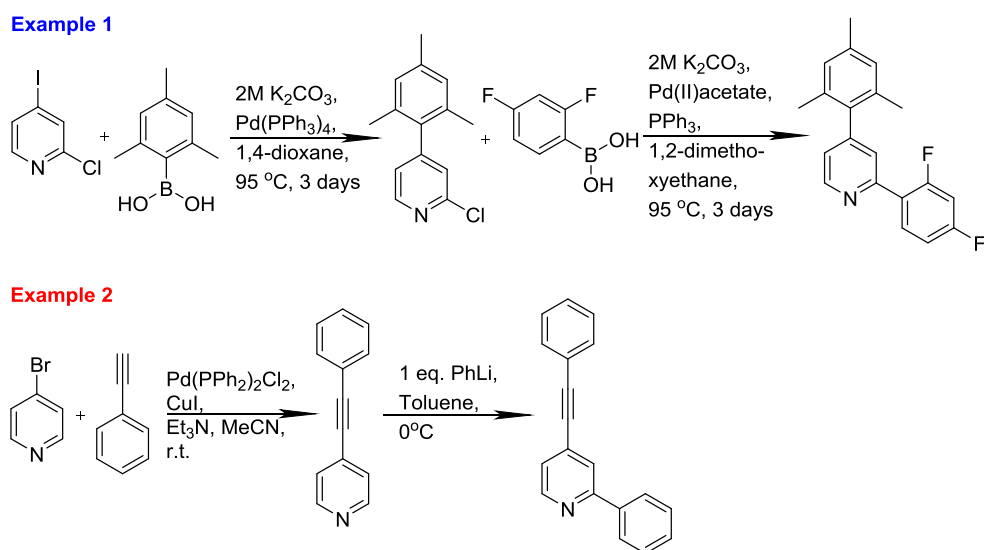
Scheme 9 *Synthesic routes to ligands used in* **example 1 and 2**

The preparing of **examples 1** and **2** employed different pathways towards the formation of the 2-phenylpyridines. **Example 1** (top one), used two Pd-catalysed reactions of 2-chloro-4-iodopyridine with mesityl boronic acid and difluoroboronic acid. In contrast, **example 2** employed the synthesis of the 4-phenylethynyl pyridine followed by the direct phenylation of the pyridine using PhLi. The high chemical reactivity of the α-proton of pyridine contributes to this reaction, and makes this substitution reaction possible.[65] Due to the commercial availability of phenyl lithium solution at reasonable price, the use of this direct phenylation step like **example 2** is worth considering. Some substituted derivatives can be made in an analogous route from readily available precursors via the preparation of substituted phenyl lithiums.

1.4 Palladium-catalysed C-C coupling reactions- background

1.4.1 Suzuki-Miyaura reaction- background

The basic information of Suzuki-Miyaura reaction has been mentioned previously. Here, the nature and mechanism of Suzuki Miyaura reaction is presented.[43]
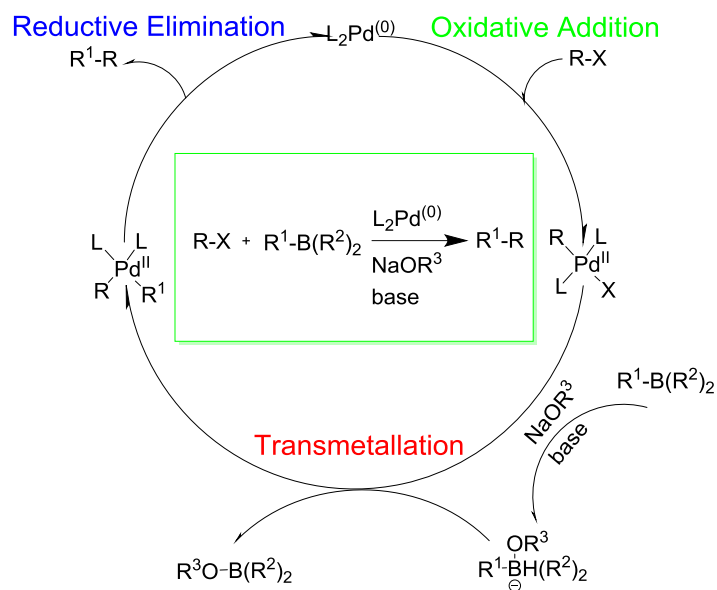
Figure 4 *A general catalytic cycle for the Suzuki-Miyaura reaction. adapted from*

reference[66]

The Suzuki-Miyaura reaction is suitable for a wide range of aryl groups. Meanwhile, aryl halides could easily obtained with iodination or bromination, aryl-boronic acid or boronates could be made from aryl halides via the aryl lithium or direct borylation. Therefore, a wide range of starting materials for the Suzuki reaction are accessible. The two significant advantages of Suzuki reaction, compared to traditional coupling reaction *e.g.* Grignard reaction or lithium reagents, is its wide choice of solvents and great tolerance of functional groups. As the nature of Suzuki reaction is an effectively S_N1 coupling reaction of the aryl halides (which hereby take the role of a source of an electrophilic carbon) and the aryl boronic acid (used as a source of a nucleophilic carbon), the reaction benefits from a polar solvent.[67] Furthermore, due to its compatibility of water, a huge range of solvents combinations can be used depending

on the solubility and stability of starting materials in specific cases. Generally, water/ methanol, water/ THF, toluene and DMF are the preferred solvent in most cases. However, due to the palladium(0) catalyst readily undergoing oxidation, an inert nitrogen atmosphere is needed to keep the catalyst in its active form. A base is also essential for the Suzuki reaction; an activity sequence has been found to be $Cs_2CO_3 > K_2CO_3 > Na_2CO_3 > Li_2CO_3$,[43] although other bases have also been applied *e.g.* *t*-BuONa [67] and CsF.

1.4.2 Sonogashira reaction- background

The Sonogashira reaction is another palladium-mediated reaction that performs a very important role in this project as well as being one of the most important C-C coupling reactions. It the most practical method in order to synthesis aryl acetylene which is able to either expand π-conjugation or continue with cyclic reaction.[68]
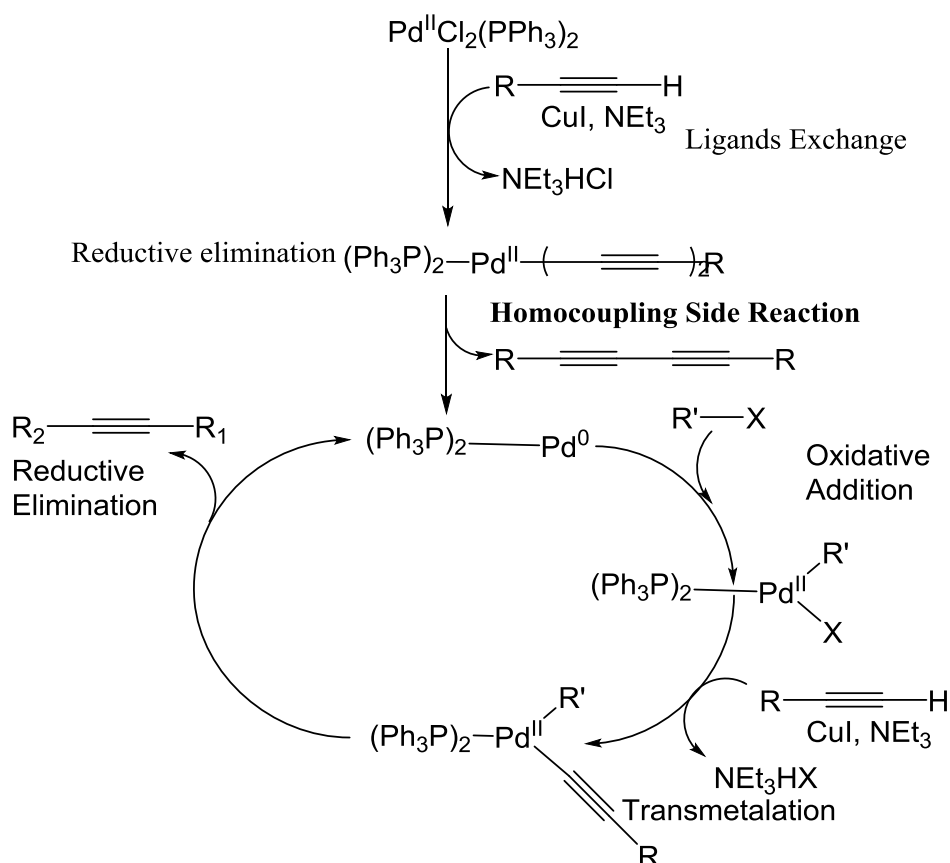
Figure 5 *A general catalytic cycle for the Sonogashira reaction. Reproduced from*

reference[69]

Sonogashira reaction is a Pd(0)-atalysed reaction, typically using a Pd(II) pro-catalyst,

$PdCl_2(PPh_3)_2$. The first step in the reaction involves the reduction of the catalyst by

excess alkyne to yield the active Pd(0) species. As a result, the homocoupling side

reaction of the alkyne is a side reaction tolerated in the Sonogashira reaction[70],

therefore in most cases, excess alkyne needs to be added, and the homocoupling by-

product could be observed in the NMR spectra. In some cases, this can be avoided by

the use of a Pd(0) catalyst *e.g.* $Pd(PPh_3)_4$, however, this is less readily handled.

Sonogashira reaction is sensitive towards both oxygen and water, however, copper-

free water-based Sonogashira reactions are currently of interest by chemists. Some progress, such as copper-free reactions, have been made.[69, 71]

1.5 Objective

In this report we seek to create a family of iridium complexes with extended aryl (phenylethynyl) substituents at the 4-postion of the pyridine rings of a Ir(ppy)$_2$XY complex. Substitution at this position will lead to prolate structures with the potential for high length/diameter ratios. By controlling the conjugation between the substituents and the pyridine rings the complexes will be able to have their emission wavelength tuned independently of the extension of the complex.

As seen above, starting with one of the simplest emissive iridium(III) complexes, Ir(ppy)$_2$(acac), the easiest way to make such complexes is to add substituents such as phenylethynyl to the 4-position of the pyridine. However, although this provides a facile means of increasing the length of the molecule, the added phenyl groups provide extended conjugation leading to red-shifted emission.[72] Therefore, in order to maintain the emission colour of the parent complex and at same time extending its length it is necessary to break the conjugation between the pyridine and the extending group. To achieve this we have included groups with steric hindrance in the backbone in order to bring about a twist of the molecule (see **Scheme 10**). Preparing complexes of this type in which the functional group R' can be further elaborated provides a versatile synthetic route to a new class of emissive iridium complex.

R= steric hindrance groups
    which are able to rotate
    rings out-of-plain, e.g. -Me
R'= phenyl-ethynyl substituents

X
| = general structure represent
Y   ancillary ligands, e.g. acac, pic
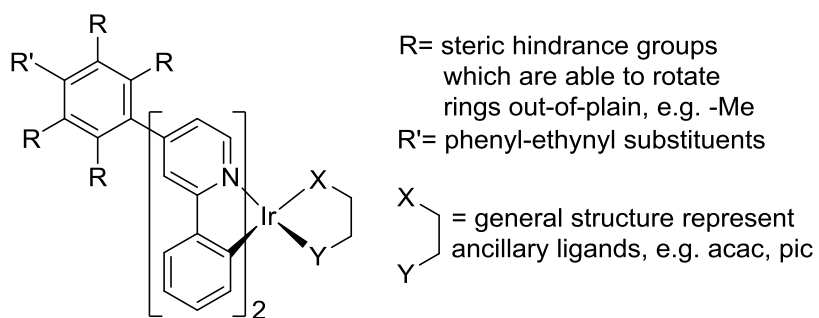
Scheme 10 *General structure of the target complexes*

Chapter 2 Synthesis results and discussion

2.1 Ligands synthesis

Scheme 11 shows the synthetic route to the target ligand **L1**; the synthesis of this ligand can be broken down into two parts, preparation of a 4-substituted pyridine and subsequent phenylation at the 2-position. Direct phenylation with PhLi makes the synthetic route more straight forward, and employs cheaper reagents. For example, 2,4-dibromo-pyridine (£50 per gram), could be used, but further reactions would require boronic acids or tin compounds to be made with the purpose of doing subsequent Suzuki reaction or Stille reactions. In that case, substituents need to be reacted with Pd catalysts and butyl lithium. R. Edkins has demonstrated that substituted phenyl lithium reagents can be made from aromatic halides and *t*-BuLi allowing the preparation of derivatives with substituents on the 2-phenyl ring.[72]

Furthermore, because C-C coupling reactions are involved, the use of dihalopyridines, *e.g.* 2-chloro-4-bromo-pyridine or 2-chloro-4-iodo-pyridine could lead to side product formation, whilst the use of the phenylation reaction as the second step effectively eliminates these undesired products. In this work commercially sourced phenyl lithium solution is employed (1.9 M in dibutyl ether). The phenylation reaction can give rise to aromatic by-products and sometimes the yield of phenylation is not as high as those obtained from classical palladium coupling reactions. However, this is offset by its convenience and relative simplicity.
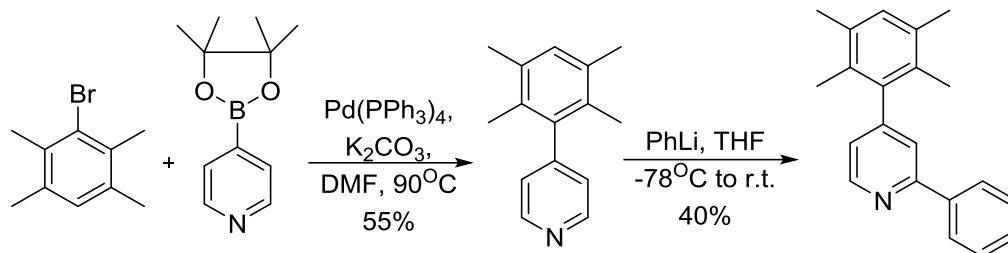
Scheme 11 *Synthesis route for **L1***

As shown in the **Scheme 12**, with the purpose of enhancing the yield of the phenylation reaction, some improvements were applied throughout experiments. Firstly, the reaction temperature has been slightly increased from 0 ℃ to room temperature (approx. 25℃). Electron-donating substituents on the pyridine ring would lead to a reduction of reactivity, thus, the reacted material is of lower reactivity comparing with starting material. Thus, excess phenyl lithium (3 equivalents) was added to enhance chemical reaction rate. Finally, because of its lower boiling point, THF was used instead of toluene. Evaporation of the reaction solvent is therefore more readily achieved. In order to inhibit side reactions, attributed to the application of higher reaction temperature and excess phenyl lithium, TLC monitoring was used to check the conversion rate of starting material, allowing the reaction to be stopped at an appropriate time. The yield has therefore been increased from 26% to average of 40%.
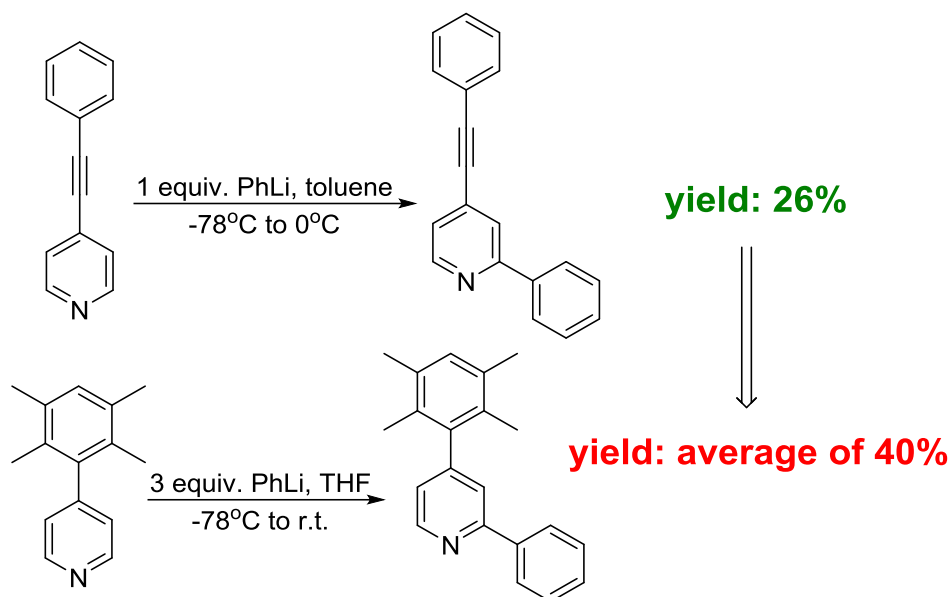
Scheme 12 *Improvements in the conditons of the phenylation reaction*

In order to prepare **L2**, the first step was to synthesis the substituted pyridine, 4-(2,3,5,6-tetramethyl-4-((triisopropylsilyl)ethynyl)phenyl)pyridine. As shown in the **Scheme 13**, from previous experience we know that triisopropylsilyl group which would protect the alkyne during phenylation is not stable under Suzuki conditions, therefore it was necessary to synthesis a mono-pyridine substituted durene with a reactive halide for a subsequent Sonogashira reaction.

reaction failed
NMR showed the deprotection of TIPS
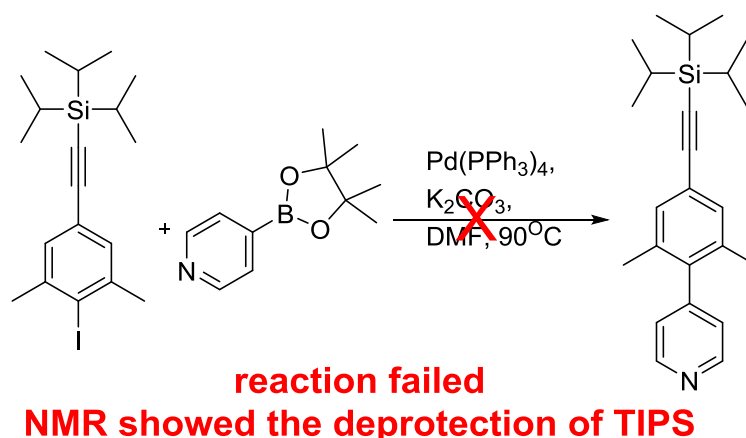
Scheme 13 *One failed example of Suzuki reaction with triisopropylsilyl ethynyl*

This was potentially difficult as halogens on both sides of durene may lead to a double Suzuki reaction. Initially, we synthesised 1-bromo-4-iodo-2,3,5,6-tetramethylbenzene (by iodinating bromodurene) and reacted this with 4-(4,4,5,5-tetramethyl-1,3,2-dioxaborolan-2-yl)pyridine under Suzuki conditions to give 4-(4-bromo-2,3,5,6-tetramethylphenyl)pyridine selectively with a yield over 60% with little purification, due to the difference in reactivity of aryl iodide and bromide. However, the Sonogashira reaction with triisopropylsilyl acetylene gave a yield of less than 20% with significant purification difficulties. This is likely due to the steric hindrance caused by the methyl groups *ortho* to the aromatic halide coupled with the lower reactivity of bromine (**Scheme 14**). Therefore to improve the yield of the Sonogashira reaction, the 4-(4-iodo-2,3,5,6-tetramethylphenyl)pyridine was used.
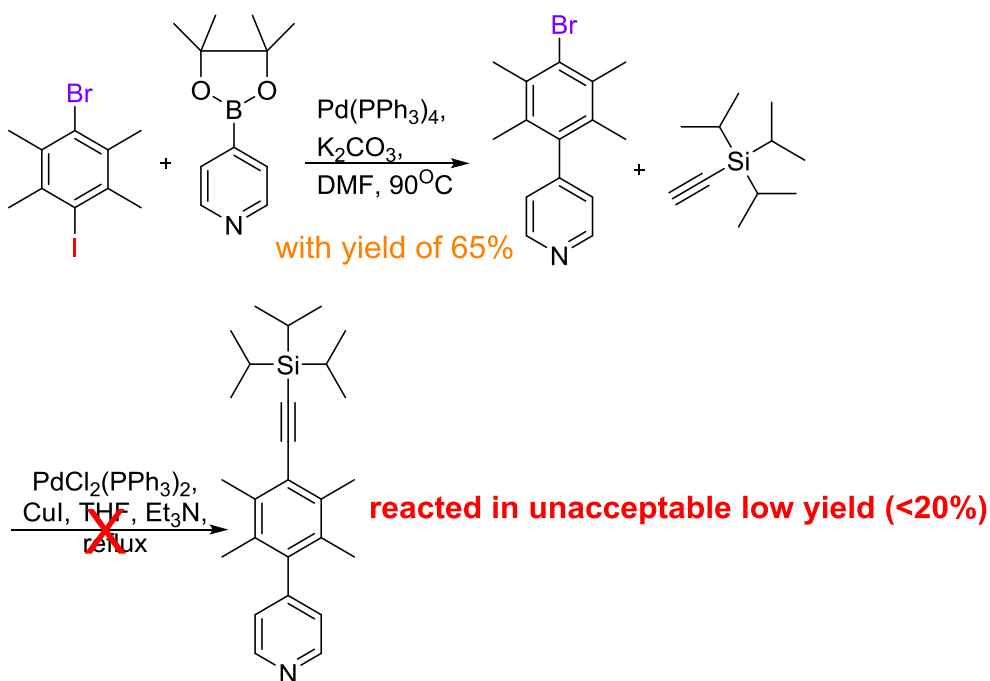
Scheme 14 *Failed 1-bromo-4-iodo-2,3,5,6-tetramethylbenzene route*

To produce this 1,4-diiodo-2,3,5,6-tetramethylbenzene was used in place of 4-bromo-2,3,5,6-tetramethylbenzene. Because, 1,4-diiodo-2,3,5,6-tetramethylbenzene, has no selectivity between sites, the Suzuki reaction was performed with three equivalents of 1,4-diiodo-

2,3,5,6-tetramethylbenzene to one of 4-(4,4,5,5-tetramethyl-1,3,2-dioxaborolan-2-yl)pyridine with the temperature strictly maintained at 90 ℃.[73] Despite the excess residual 1,4-diiodo-2,3,5,6-tetramethylbenzene the product was readily purified to give 4-(4-iodo-2,3,5,6-tetramethylphenyl)pyridine with a yield of 50%.

Even with the use of an iodo group in place of the bromo group the Sonogashira reaction still required heating to 50 ℃ to achieve appreciable yields (85%), although this is not unprecedented: similar behaviour that has been reported with sterically hindered iodo aromatics. According to Benstead, Michael, *et al.*,[74] sterically hindered Sonogashira reactions give low yields, but improved reaction rates and yields could be obtained by heating the reaction.

The phenylation to give **L2** produced with relatively low yield (35%) and required significant purification. The reason for the difference in this behaviour as compared to 2-phenyl-4-(2,3,5,6-tetramethylphenyl)pyridine was not clear.
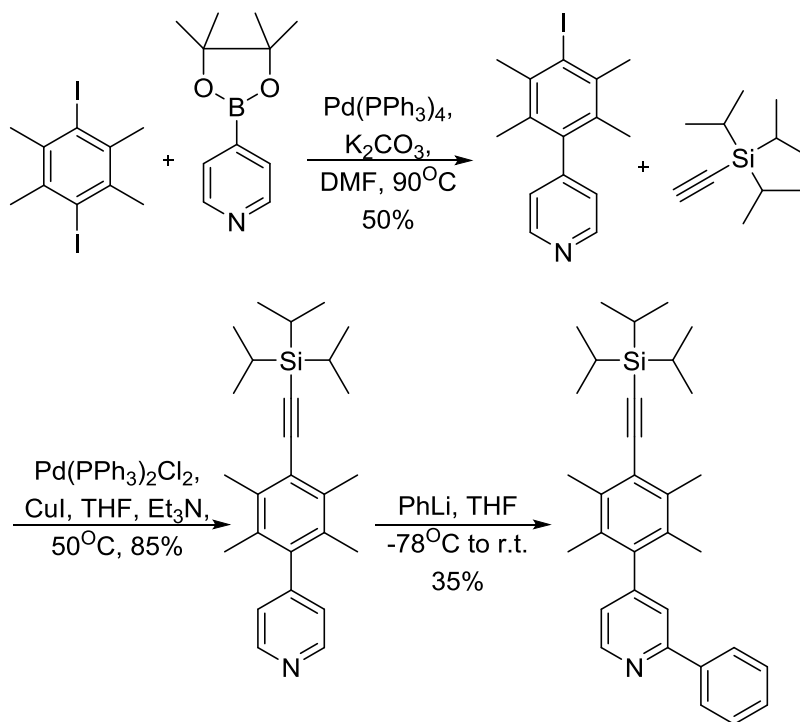
Scheme 15 *Final synthesis route for L2*

2.1.1 Crystallography

An X-Ray diffraction study showed that 4-(2,3,5,6-tetramethylphenyl)pyridine has an orthorhombic crystal structure and crystallises in a space group Pnma with one molecule of 4-(2,3,5,6-tetramethylphenyl)pyridine per unit cell (see **Figure 6**). The structure consisting of one pyridine ring with a duryl ring attached at the para-position of the pyridine (C3) is consistent with NMR spectroscopy and mass spectrometry. The torsion angle between the rings of -90.67(134) ° (C2-C3^C6-C7). This twist is the results of the aromatic rings minimising the steric hindrance caused by the *ortho*-methyl groups (C10). Meanwhile, this C3-C6 bond does have a longer bond length, 1.496(18) Å, comparing with other to normal C-C bonds with sp^2 hybrid orbital (usually approximately 1.34 Å).[75]

33
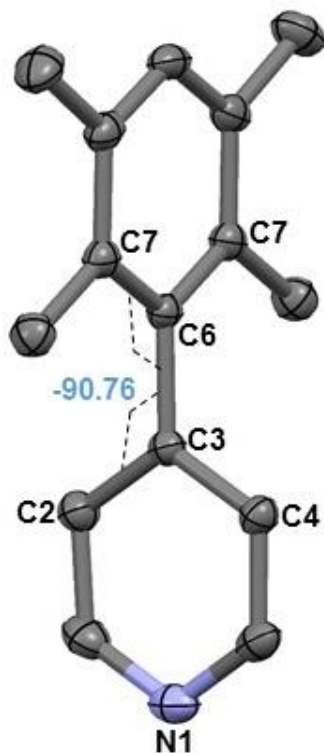
Figure 6 *Molecular structure of 4-(2,3,5,6-tetramethylphenyl)pyridine*

(ORTEP drawing at 50% ellipsoid probability)

An X-Ray diffraction study showed that 4-(2,3,5,6-tetramethyl-4-((triisopropylsilyl) ethynyl)phenyl)pyridine has a triclinic crystal structure and crystallises in space group P-1 with one molecule of 4-(2,3,5,6-tetramethyl-4-((triisopropylsoly)ethynyl)phenyl)pyridine per unit cell. The structure consists of one pyridine and a triisopropylacetylene group attached in para-positions to a durene ring, which is out-of-plane, rotated -90.18(3) ° relative to the pyridine ring, measured by torsion angle C4-C3^C6-C7. As shown in the crystal structure, similar as 4-(2,3,5,6-tetramethylphenyl)pyridine, the C3-C6 bond is twisted in order to minimize the steric hindrance effect of *ortho*-methyl groups. One silicone could be observed, attached with ethynyl C17, and connected to the three isopropyl groups. The crystal structure also confirms that the molecule is linked in a linear fashion. This structure is consistent with the NMR spectroscopy and mass spectrometry data obtained.
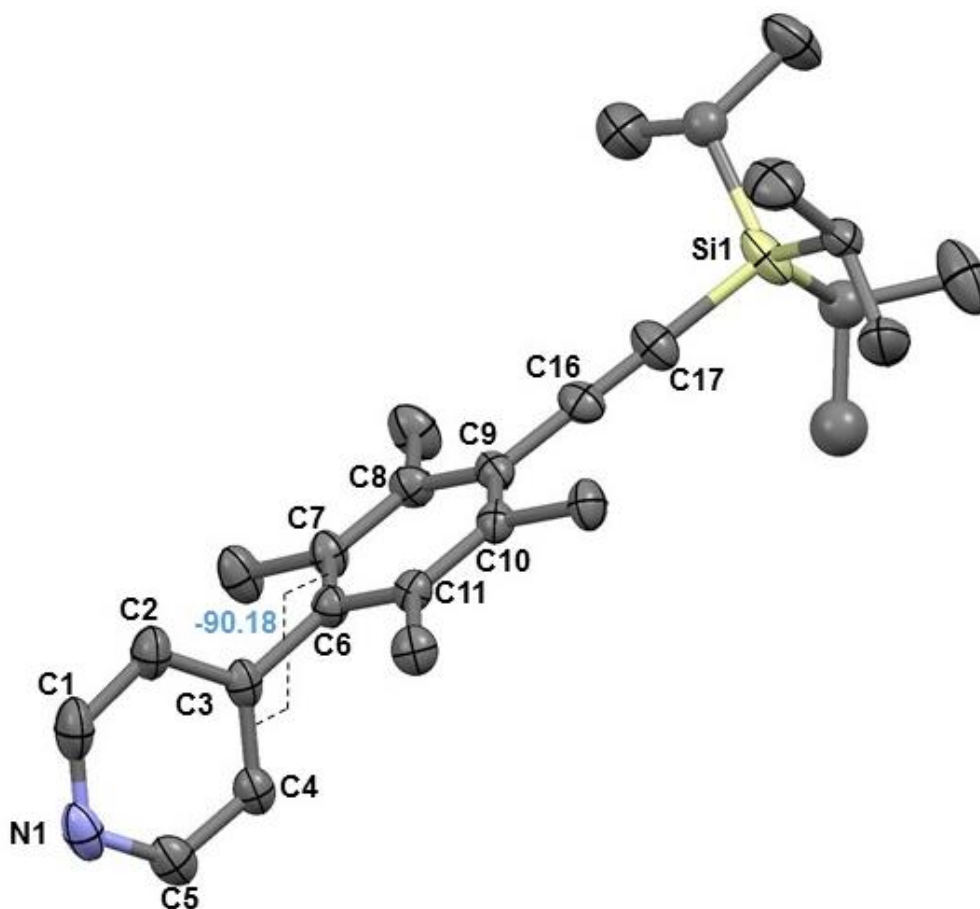
Figure 7 *Molecular structure of 4-(2,3,5,6-tetramethyl-4-*

((triisopropylsoly)ethynyl)phenyl)pyridine

(ORTEP drawing at 50% ellipsoid probability)

An X-Ray diffraction crystallography showed that **L1** has a monoclinic crystal structure and crystallises in a space group P2$_1$/n with one molecule of **L1** per unit cell. The structure consists of one pyridine, one phenyl along and one duryl ring, with the duryl ring out-of-plane, rotated -102.86(17)° out of plane relative to the pyridine, measured by torsion angle C2-C1^C6-C7. As shown in the crystal structure, same as 4-(2,3,5,6-tetramethylphenyl)

pyridine, the C1-C6 bond is twisted in order to minimize the steric hindrance effect conferred by the *ortho*-methyl groups. The C3-C16 bond linking the phenyl ring and pyridyl ring together, twisted a smaller amount (32.18(2)°). This structure is consistent with the NMR spectroscopy and mass spectrometry data obtained.
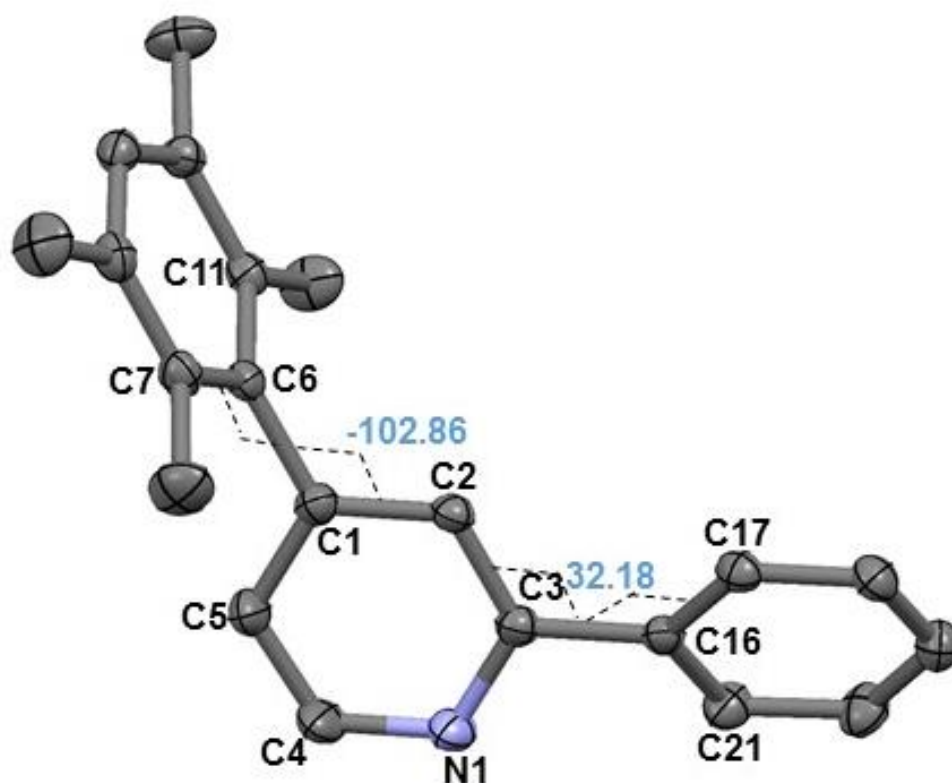
Figure 8 *Molecular structure of **L1** (ORTEP drawing at 50% ellipsoid probability)*

2.1.2 Conclusion

In conclusion, two novel ligands (**L1** and **L2**) were synthesised by a combination of Suzuki, phenylation and Sonogashira reactions and characterised using ^{1}H-, ^{13}C-NMR, mass-spectrometry and elemental analysis. Each of the reactions were optimised by exploring

various synthetic routes to give the highest yields with the simplest purification. Additionally, crystal structures were obtained for 4-(2,3,5,6-tetramethylphenyl)pyridine, 4-(2,3,5,6-tetramethyl-4-(triisopropylsilyl)ethynyl)phenyl) pyridine and **L1** which confirm the addition of the methyl groups that causes the phenyl group rotate out of plane with the pyridine ring by approx. 90° and hence will break the π-conjugation. Ligands **L1** and **L2** will be used in Chapter 2.2 to coordinated to iridium.

2.2 Complexation

Complexation reactions in this project are based on a general two-step iridium method commonly employed. Thus, $IrCl_3 \cdot xH_2O$ was reacted with the respective ligand (**L1** or **L2**) to generate a chloro-bridged Ir(III) dimer, $(IrL_2)Cl_2$. The dimer was then reacted with the ancillary ligand resulting in a *bis*-cyclometalated iridium complex, IrL_2XY.

In our experiments, the dimer was not isolated or purified, rather it was precipitated as a crude material and reacted on with the respective ancillary ligand acetylacetonate (acac) or picolinate (pic) and the final product was purified by chromatography. Although mass-spectrometry and NMR spectroscopy indicated the presence of **C5** in the solution, it was not possible to be isolate it as a pure product, largely due to the high polarity of the complex making it difficult to be purified by chromatography. Therefore, further work on pic-based complexes was abandoned. The acac-based complexes, however, were readily isolated as pure compounds for both **C1** and **C2** (see **Scheme 16**), and were characterised by NMR spectroscopy, mass spectrometry and elemental analysis.
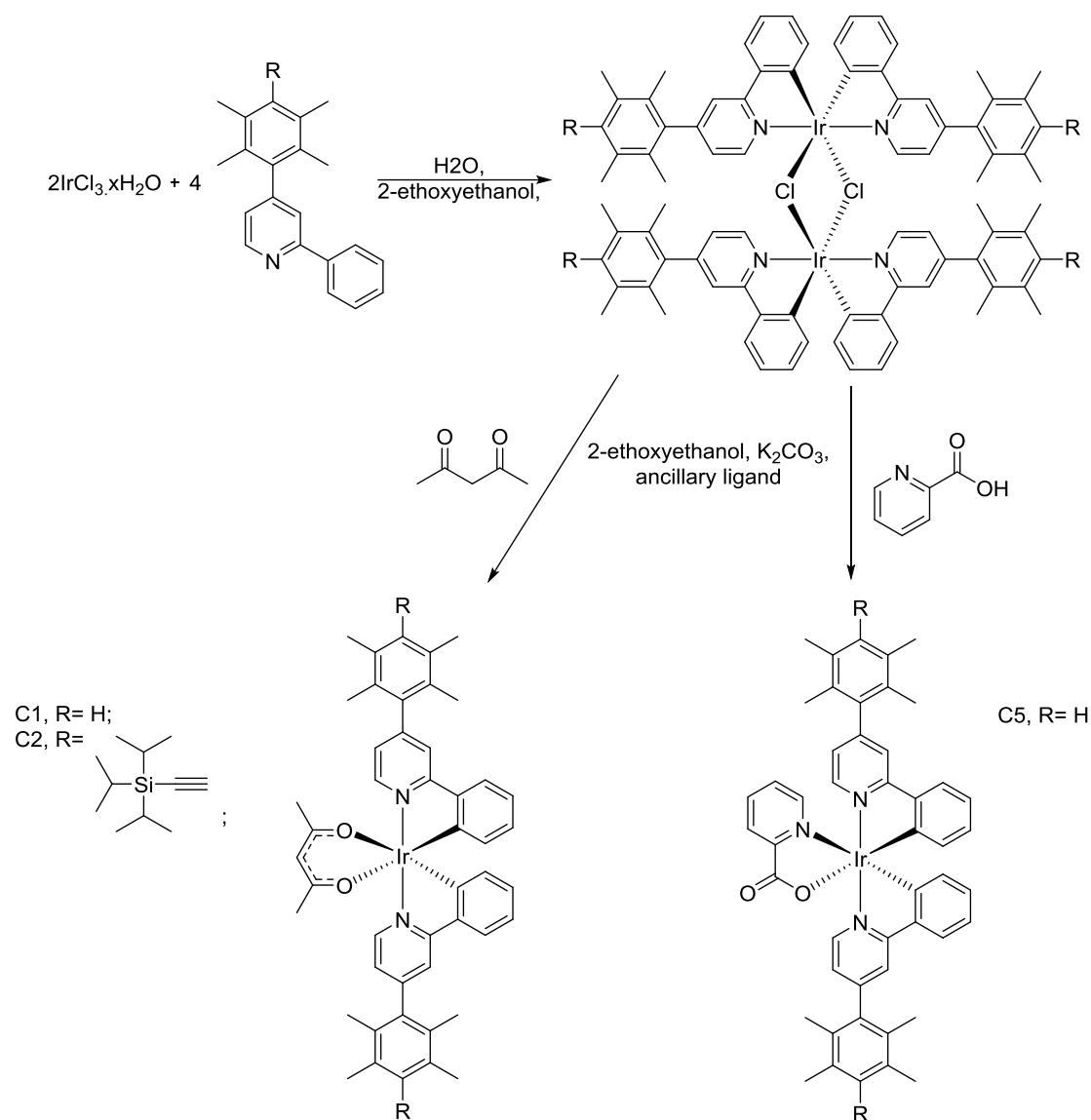
Scheme 16 *General complexation reaction*

2.2.1 Crystallography

An X-Ray diffraction crystallography showed that **C1** has a orthorhombic crystal structure

and crystallises in a space group Pbcn with one molecule of **C1** per unit cell. The structure

consists of one Ir(III) metal ion in an octahedral geometry complexed to two bidentate 2-

phenyl-4-(2,3,5,6-tetramethylphenyl)pyridine (**L1**) ligands, with the pyridine moieties of **L1**

trans to one another. The remaining coordination sites were occupied by the ancillary ligand

acac. The duryl ring was rotated out-of-plane 109.23(6)° (C2-C3^C12-C17) and 91.20(7)° (C32-C33^C42-C43). As shown in the crystal structure, same as the ligand **L1**, the C1-C6 bond is twisted in order to minimize the steric hindrance effect built by the *ortho*-methyl groups. Meanwhile, as measured in **Figure 8**, the torsion angle (N1-C5^C6-C7) was twisted by 5.71(6)° which suggested that the C5-C6 bond is of slightly rotated. The torsion angle between pyridyl and phenyl ring is still slightly larger than observed in other cyclometalated iridium complexes *e.g.* Ir(ppy)$_2$(acac) of 1.96° (reported by Lamansky, Sergey, *et al.*).[17] The crystal structure also shows the linear arrangement of the two ligands about the metal centre. When it comes to the iridium metal centre, related bond lengths were measured to prove whether the core complex has been altered or not. As reported in the previous paper, distances between iridium and nitrogens, oxygens and carbons in Ir(ppy)$_2$(acac) have been measured as 2.010Å, 2.146Å and 2.003Å respectively.[17] In terms of **C1**, related bond lengths are given in the **Table 3**. Based on these data, the bond lengths between the central iridium atom and the bound ligands were hardly changed, showing that the structure of the core cyclometalated complex has not been significantly altered. This structure is consistent with the NMR spectroscopy and mass spectrometry data obtained.
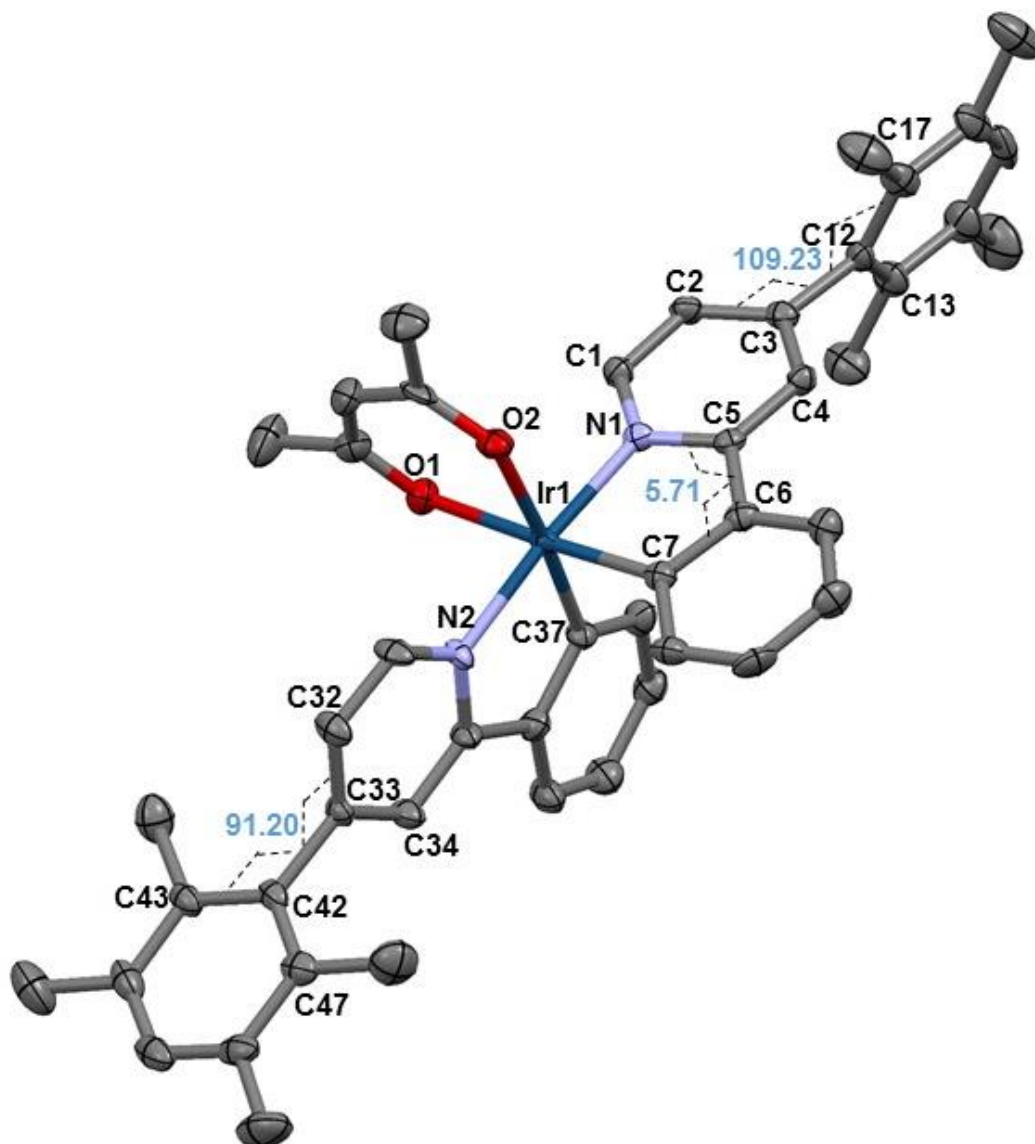
Figure 9 *Molecular structure of **C1** (ORTEP drawing at 50% ellipsoid probability)*

Bond	Length **C1**/ Å	Length Ir(ppy)$_2$(acac)/ Å
Ir1-O1	2.155(4)	2.146
Ir1-O2	2.147(3)	
Ir1-N1	2.026(4)	2.010
Ir1-N2	2.032(4)	
Ir1-C7	1.991(5)	2.003
Ir1-C37	1.999(5)	

Table 4 *Bond lengths between iridium and ligands in C1*

2.2.2 Conclusion

In conclusion, two ligands (**L1** and **L2**) were reacted iridium chloride to form different iridium μ-chlorodimers, and these reacrted on with two different ancillary ligands (acac and pic). These reactions yielded four different Ir(L$_2$)(XY) type *bis*-cyclometalated iridium complexes. Although the complex **C5** was synthesised, it could not be isolated as a pure material. However, the acac based complexes **C1** and **C2** were readily synthesised, purified and characterised by ^{1}H-, ^{13}C-NMR spectroscopy, mass-spectrometry and elemental analysis. Additionally, the crystal structure of **C1** showed that the core of the complex was consistent with other non-modified complexes and that the durene ring was rotated nearly 90℃ out-of-plane.

2.3 Modification of iridium complex C2: Deprotection and Extension

The complexes **C3** and **C4** could be made either from the preparation of a complete appropriate ligand and reacting this with iridium chloride, or by the deprotection and subsequent Sonogashira coupling of complex **C2**. Both routes are expected to be challenging. The main factor that contributed to our choice of reaction pathway was a consideration of the solubility of reactants and intermediates. In many previous cases, the extension of highly conjugated aromatic systems leads to poor solubility due to strong solid-state packing. While the reactions themselves should not be problematic, work-up and chromatography may become difficult. As a result, although *tert*-butyl has been used to increase solubility of this kind of molecules, we elected to introduce this functionality later in the synthesis. Based on this theory, **C2** was modified by de-protection and a Sonogashira reaction with 1-(*tert*-butyl)-4-((4-iodophenyl)ethynyl)benzene and 1-(*tert*-butyl)-4-iodobenzene, as illustrated in **Scheme 17**. At the beginning, all of those Sonogashira reactions turned out low yields with TLC suggesting that this was due to the starting materials not reacting. It should be mentioned, at that moment, all Sonogashira reactions were run under so called "normal" condition. $PdCl_2(PPh_3)_2$, NEt_3, THF and CuI were used and the reaction mixtures were stirred overnight at room temperature. In this case, we assumed that steric hindrance may decrease the reaction rate. After that, some small scale reactions were set up at 50-60℃, and, successfully gave the product with high yield (approx. 80%). Pure products were obtained by chromatography (silica/ DCM) and precipitation with methanol.

TBAF Deprotection

alkynyl intermediate

Sonogashira with different R groups

C3, R=

C4, R=
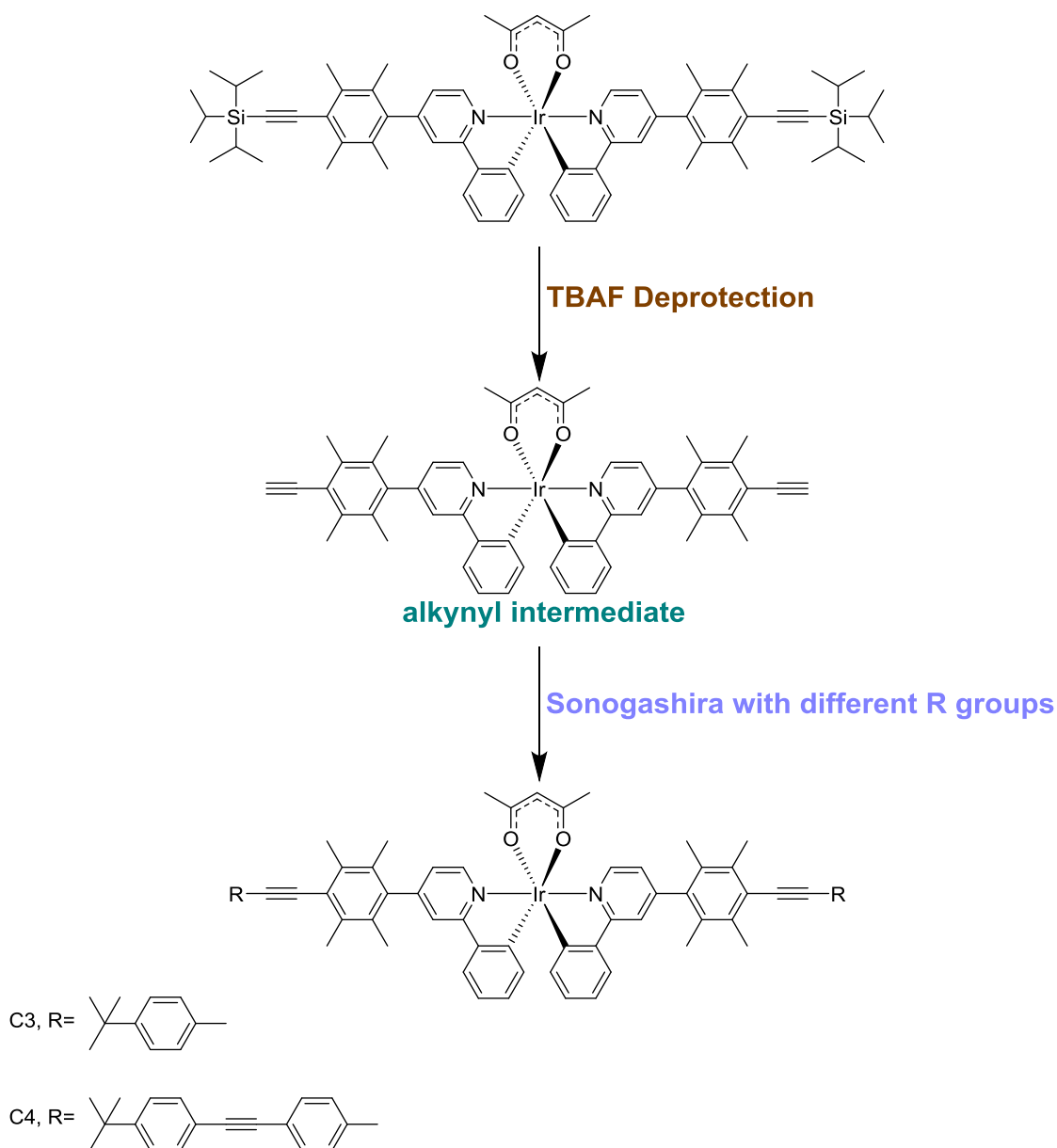
Scheme 17 *General synthesis route to modify complex **C2***

Obtaining single crystals of these extended, long iridium complexes, proved to be unexpected difficult. Although, many solvents combinations and crystallization conditions were tested, only very fine crystals were produced, and the corresponding X-ray structure determinations failed.

2.3.1 Conclusion

In conclusion, modification of iridium complexes was proven to be a productive synthetic pathway to extend the length of iridium ppy complexes along the N-Ir-N axis. Sonogashira reactions of the hindered systems proceeded in low yield under normal conditions, but upon heating the reaction enhanced yields were obtained. NMR spectroscopy and mass spectrometry data for the mateirals are consistent with the expected structures. Unfortunately, crystal structures for rest of complexes have not been obtained so far.

2.4 Attempt to synthesis phenyl-duryl substituted series
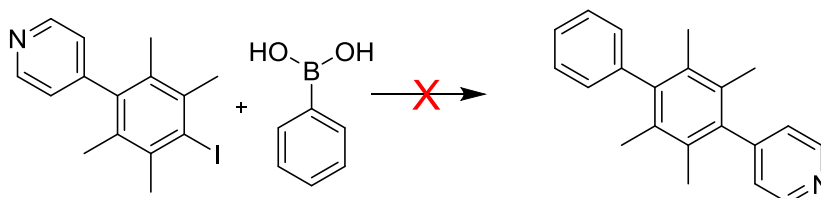
Scheme 18 *One failed attempt of making 4-(2,3,5,6-tetramethyl-[1,1'-biphenyl]-4-yl)pyridine*

Apart from those complexes, a different series of complexes with their novel 2-phenyl-4-(2,3,5,6-tetramethyl-[1,1'-biphenyl]-4-yl)pyridine ligand have also been studied. Surprisingly this complex, containing a number of aromatic rings, has great solubility in almost any organic solvents from non-polar hexane to polar methanol. This property is certainly a great advantage in terms of solvent-processing film preparation, but also presents difficulties when it comes to its purification. Because of the steric hindrance, the Suzuki reaction never went with 100% conversion ratio, there would always remain some of the starting material. The desired product, 4-(2,3,5,6-tetramethyl-[1,1'-biphenyl]-4-yl)pyridine, has very similar polarity to the starting material, 4-(4-iodo-2,3,5,6-tetramethylphenyl)pyridine. In this case,

recrystallization and precipitation as salt have been tried as well as chromatography. Finally, this way was abandoned by us.

We found that, due to the existence of pyridyl, both the starting material and the product require quite polar solvent combination like 20% ethyl acetate in hexane to elute on silica. In this case, the difference between phenyl and iodo substitutions cannot afford a good separation between starting material and product. But if we reverse the order of the two couplings, that is first react diiododurene with benzene boronic acid, a simple hexane/ silica chromatography would be able to separate the reaction mixture, yielding the pure intermediate 4-iodo-2,3,5,6-tetramethyl-1,1'-biphenyl. Using this method, we finally succeeded in synthesis 4-(2,3,5,6-tetramethyl-[1,1'-biphenyl]-4-yl)pyridine.
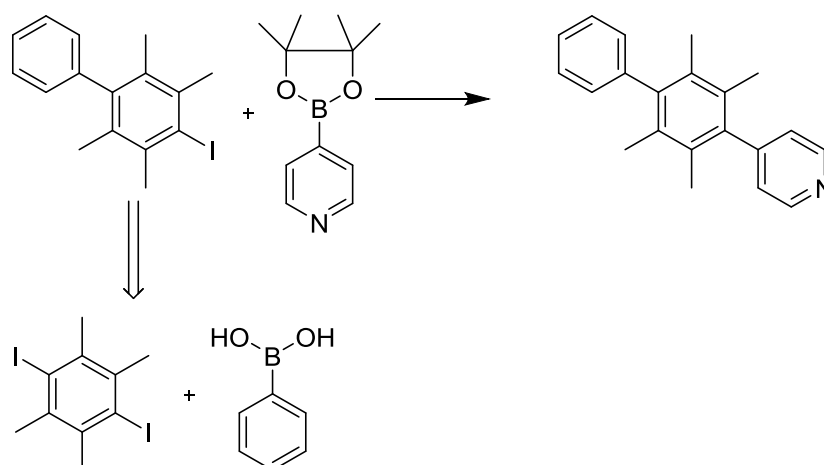
Scheme 19 *Synthetic route towards 4-(2,3,5,6-tetramethyl-[1,1'-biphenyl]-4-yl)pyridine and disconnection of 4-iodo-2,3,5,6-tetramethyl-1,1'-biphenyl*

However, the reaction 4-(2,3,5,6-tetramethyl-[1,1'-biphenyl]-4-yl)pyridine with phenyl lithium yielded a number of aromatic by-products, and NMR suggested the presence of bipyridyl derivatives. The typical purification procedure for these phenylation reactions is a pre-chromatography of the reaction mixture followed by precipitation of the product as its

HCl salt which is washed with hexane and diethyl ether. We are able to get rid of many impurities with these processes, but it does not allow pyridyl derivatives to be readily removed. Although the final ligand of this series has not been successfully prepared, the crystal structure of the important intermediate 4-(2,3,5,6-tetramethyl-[1,1'-biphenyl]-4-yl)pyridine was obtained allowing the structure of this compound to be determined. The crystal structure clearly shows the unique spatial configuration that the ortho-methyl groups twisted C-C bonds of both side and therefore made the duryl ring out-of-plane.
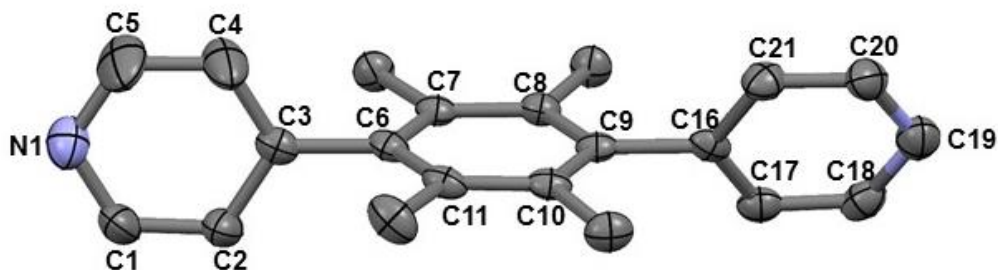

Figure 10 *Crystal structure of 4-(2,3,5,6-tetramethyl-[1,1'-biphenyl]-4-yl)pyridine*

(ORTEP drawing at 50% ellipsoid probability)

Chapter 3 Photophysics and computational study

As mentioned in the prior literature review section, introduction of aromatic substituents on to the 4-position of the pyridine may lead to a distinct red-shift. However, as the 4-substituent is oriented out-of-plane, the π-conjugation would be blocked, and the red-shift normally associated with extended π-conjugation would not occur. This project is mainly concerned with investigating how the steric hindrance induced by *o*-methyl groups affects the π-conjugation. In this case, the photophysical properties, emission spectrum, lifetime and photoluminescence quantum yield (PLQY) of the prepared complexes should be compared to the Ir(ppy)$_2$(acac) and to derivatives lacking the *o*-methyl functionalise.

3.1 Electronic absorption spectrum of target complexes C1-4

As shown in figure 12, the absorption spectrum of these four cyclometalated iridium complexes are different to each other. **C1** gives rise to a strong absorption below 320 nm, reflecting the π-π* ^{1}LC bands, with relatively weak peaks at 340-500 nm consisting of ^{1}MLCT, ^{3}LC and ^{3}MLCT bands. As discussed in the previous chapter, strong SOC (spin-orbit coupling) relaxes the forbidden singlet-triplet transition allowing absorption bands to the ^{3}LC and ^{3}MLCT states. As a result, those bands could be observed in both the absorption and excitation spectrum, although they are weaker than π-π* ^{1}LC bands. The additional ethynyl TIPS functionality in **C2** compared to **C1** results in a 20 nm red-shift of the π-π* ^{1}LC bands at ca. 300 nm, while the ^{1}MLCT, ^{3}LC and ^{3}MLCT bands could still be found in the spectra between 340-500 nm. Due to the conjugated phenyl ethynyl chain, the π-π* ^{1}LC bands of **C3** became more complex while the other bands are similar as **C1** and **C2**. The metal dominated absorption bands, ^{1}MLCT, ^{3}LC and ^{3}MLCT, showed little difference between the complexes, but the π-π* bands (297-316 nm) showed significant differences. We attribute this difference

47

to the inclusion of the twist in the backbone of the complexes due to the durene ring. In terms of **C4**, the conjugated long chain ((4-phenylethynylphenyl)ethynyl) has a pronounced new band in the absorption spectrum extending up to ca 360 nm, attributed to the presence of the bis(1,4-phenylethynyl)benzene motif. The further reduction of the energy level of π^* orbital made the **C4** π-π^* [1]LC bands red-shifted to where the [1]MLCTs of **C1-3** are. In this case, [1]MLCT, [3]LC and [3]MLCT bands are hard to assign, they are actually even hardly presented, and we assume charge transfer events at excited states are complicated.
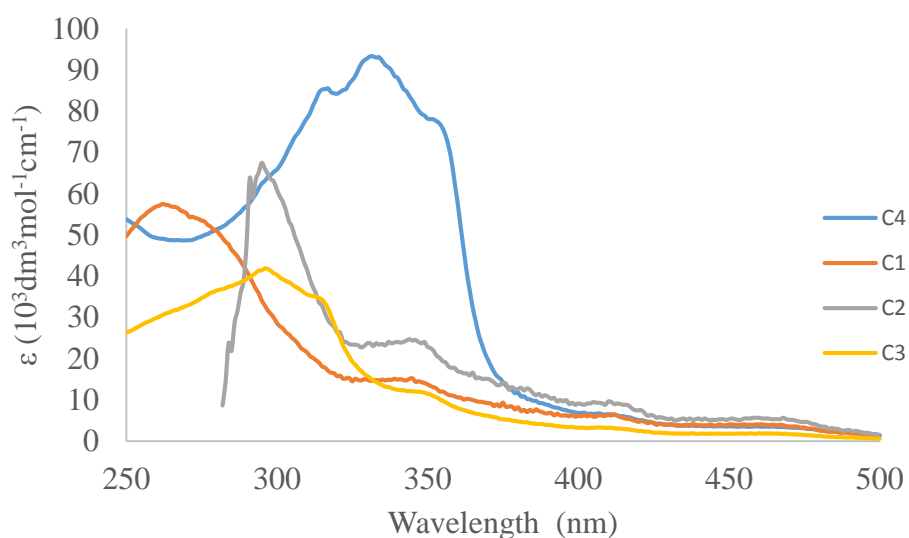

Figure 11 *Absorption spectrum of target complexes **C1-4** in DCM, the intensity are*

normalized accordingly versus extinction coefficient

Complex	absorption λ/ nm(ε/ 10^3dm^{3}mol^{-1}cm^{-1})
C1	262(57.5), 345(34.5), 410(17.4)
C2	297(64.8), 348(34.9), 414(12.8), 470(7.8)
C3	297(41.7), 316(36.3), 352(12.4), 413(3.51), 469(2.05)
C4	316(84.7), 333(92.5), 354(76.3), 390(9.46), 412(6.86), 469(3.58)

Table 5 *Extinction coefficient of target complexes **C1-4** measured as solution in DCM*

The complex Ir(dppy)$_3$ has similar structure to **C1**, in that both of **C1** and Ir(dppy)$_3$ contain 2,4-diphenyl pyridine ligands. However the introduction of the sterically demanding methyl groups in **C1** twist the 4-phenyl group, and the π-conjugation is blocked. In the case of Ir(dppy)$_3$, the introduction of phenyl group on the 4-position of pyridine extends the π-conjugation, making the absorption spectra significantly red-shifted compared to Ir(ppy)$_2$(acac), as shown in **Figure 12**. Broad intense bands could be observed between 280 nm and 400 nm which reflected the complex charge transfer among the iridium metal centre, ppy ligands and phenyl substituents. Bands corresponding to π-π^* ^{1}LC, ^{1}MLCT, ^{3}LC and ^{3}MLCT cannot be assigned clearly as Ir(ppy)$_2$(acac). On the contrary, by rotating the substituent out of plane, the extension of π-conjugation has been minimized, making the absorption spectra of **C1** similar to Ir(ppy)$_2$(acac). Both the position and extinction coefficient of **C1** are hardly changed. However, π-π^* ^{1}LC bands of **C1** broadened somehow, and that is the only visible difference of absorption spectra of these two complexes.
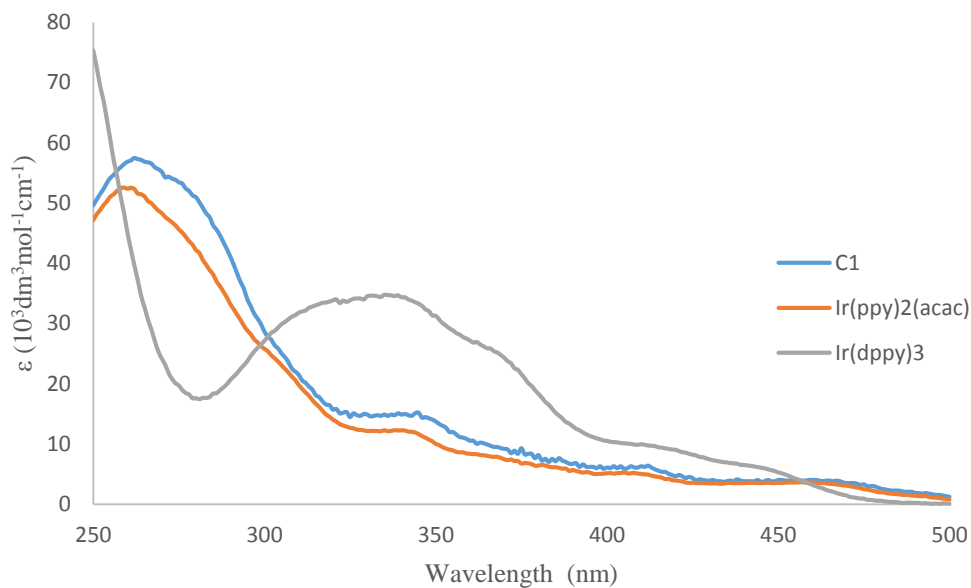
Figure 12 *Comparison of absorption spectra between **C1**, Ir(ppy)$_2$(acac) and Ir(dppy)$_3$, measured in DCM solution*

3.2 Emission spectra, PLQY and lifetime of target complexes C1-4

The emission spectra of the related four complexes, **C1** (519 nm), **C2** (522 nm), **C3** (527nm) and **C4** (526 nm), are nearly the same. The emission properties are however, significantly different to each other in luminescence lifetime and PLQY.
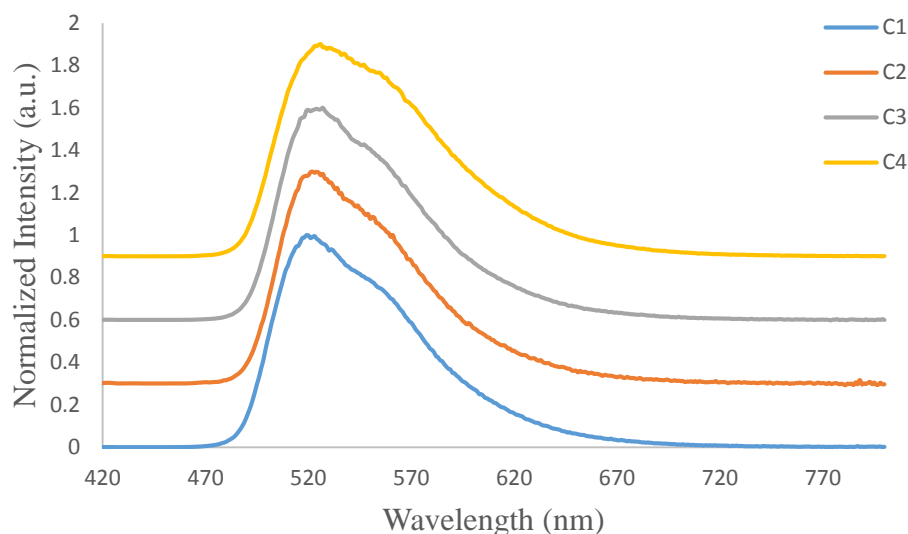
Figure 13 *Emission spectrum of target complexes **C1-4** in DCM*

The luminescence lifetime of cyclometalated iridium complexes is typically of the order of 1-10μs, and as shown in the table 5, the luminescence lifetimes of **C1-3** (approximately 1μs) in degassed solvent are similar. In the case of **C4** (15.4μs), not only is the absorption/ excitation spectrum red-shifted, but also the photoluminescence lifetime (τ) is distinctly larger than expected, τ_p =15.4μs, and the pure radiative lifetime of **C4,** τ_0=37.6μs, being beyond the typical value measured for iridium complexes. The reason could be complex. Denisov S A, Cudré Y, Verwilst P, *et al* indicated that when the aromatic substituents have similar triplet energy level as emissive triplet metal-to-ligand charge-transfer (^{3}MLCT) state, excited-state equilibration is established as a result of reversible electronic energy transfer (REET) leading to a delayed emission.[76] Furthermore, because the triplet energy level of BPB (485 nm)[77] is similar as the ^{3}MLCT (460 nm) of the Ir(ppy)$_2$(acac)[17], it is possible that **C4** could be exhibiting this REET behaviour.

Complex	$\tau_p/\mu s$	PLQY	$\tau_0/\mu s$	$\lambda_{EM}\,/\,nm$
Ir(ppy)$_2$(acac)	1.6	0.34	4.7	516
Ir(dppy)$_3$	N/A	N/A	N/A	585
C1	1.2	0.56	2.1	519
C2	1.0	0.56	1.8	522
C3	1.2	0.39	3.1	527
C4	15.4	0.41	37.6	526

Table 6 *Emission properties of target complexes **C1-4** and Ir(dppy)$_3$ in degassed DCM solution, values of Ir(ppy)$_2$(acac) is adapted from reference[11]; τ_0, is so called pure radiative lifetime, measured by τ_p/Φ_p*
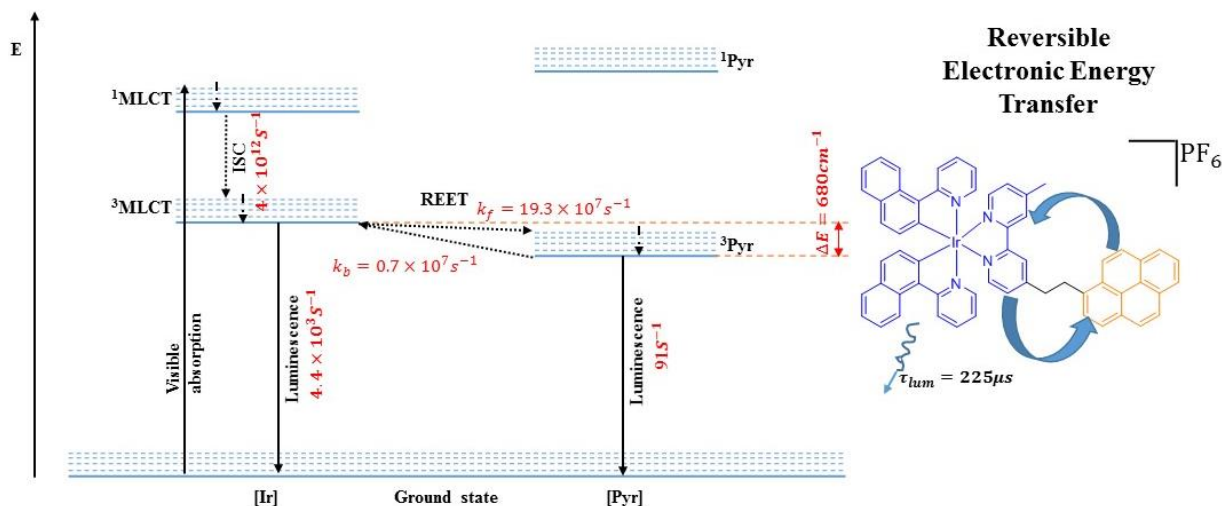
Figure 14 *The nature of reversible electronic energy transfer (REEF), diagram reproduced from reference*[76]

The PLQY of **C1** and **C2** are approximately 16% higher than Ir(ppy)$_2$(acac). The explanation of the enhancement of PLQY is still not clear. To be more specific, the duryl ring, although not conjugated with pyridine, would still contribute to the charge-transfer processes, and therefore, the activated the metal centre should still engage in MLCT charge transfer. However, **C3** and **C4** turned out to have relatively lower PLQYs, approximately 40%. We propose that the reason, for this phenomenon is attributed to the increased non-radiative decay pathways made possible by the increased vibrational and rotational modes associated with the increased size of the molecule. Nevertheless PLQY can have a range of complicated factors and may not be the result of one particular aspect.
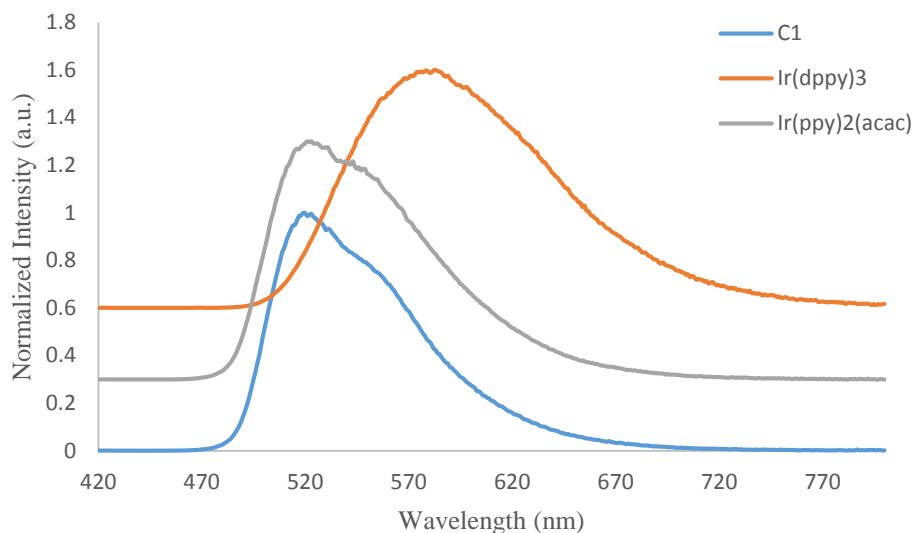
Figure 15 *Comparison of emission spectra between **C1**, Ir(ppy)₂(acac) and Ir(dppy)₃, measured in degassed DCM solution*

Further comparison with Ir(ppy)₂(acac) and Ir(dppy)₃ in their emission spectra shows the significant effect of rotating aromatic substituent out of plane. Both **C1** and Ir(dppy)₃ are constructed with cyclometalated 4-substituted-2-phenyl-pyridine ligands, and their chemical structures are similar. However, with the introduction of methyl groups at the 4-substituted phenyl group, the emission spectrum of **C1** does not red-shift as much as Ir(dppy)₃. As shown in the CIE Chromaticity Diagram as well as photograph taken in the black case with UV light source, the emission colours of those four Iridium complexes are hardly distinguished. These light emitting materials are therefore referred to be typical green emitters just like Ir(ppy)₂(acac). In the contrary, the Ir(dppy)₃ is red-shifted, due to the expansion of π-conjugation, has become a yellow emitter according to the CIE chromaticity diagram.
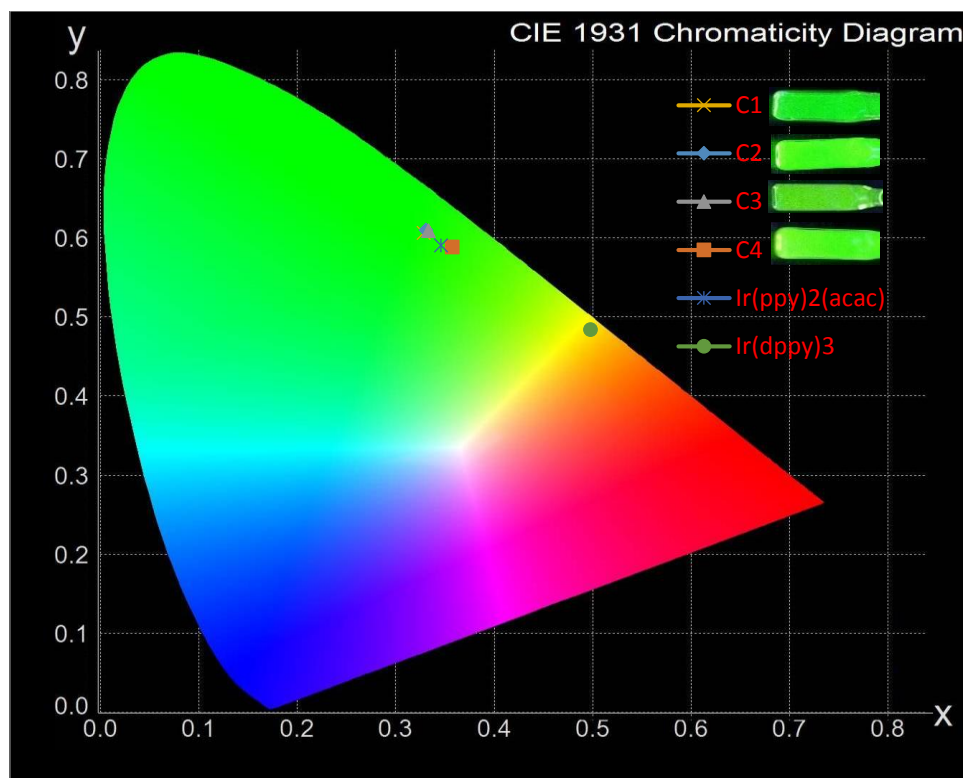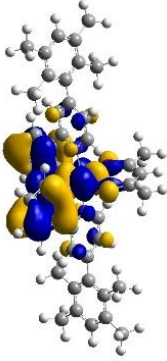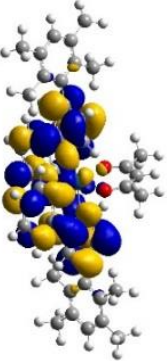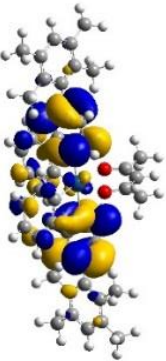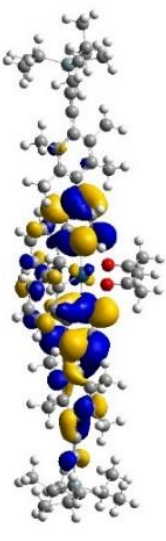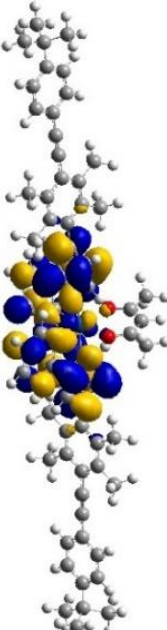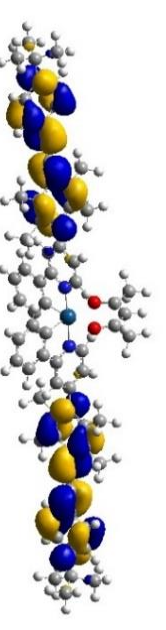
Figure 16 *CIE Chromaticity Diagram and photograph taken in the black case with UV light source*[78]

3.3 Computational study of C1-4 and related complexes

In order to gain insight to emission behaviour observed for the complexes, density functional theory (DFT) calculations were performed by Dr Ross Davidson. The calculations were performed using a B3LYP functional with a SDD basis set, optimising the complexes in a SCRF(DCM) solvent field. The frontier molecular orbitals, energy levels and bandgap are given in the table below. As presented in the table, in terms of **C1-3**, the HOMOs of these three complexes are located on the metal centre phenyl part of the ppy ligand. The LUMOs lie predominantly on the pyridyl part of ppy with hardly any contribution from the duryl or attached phenylethynyl groups respectively. The calculation confirm that the ortho-methyl groups twist the ring out of plane, therefore, the π-conjugation between two rings is broken. When it comes to **C4**, the HOMO was located on the metal centre and phenyl part of ppy,

while the two degenerate LUMOs were located on the extended phenyl acetylene oligomer. The energy level of this part (-1.82 eV) is lower than the LUMO+2 which is located on the pyridyl part of ppy (-1.47 eV). The DFT calculations showed that the HOMO, LUMO (LUMO+1) and LUMO+2 are located on different part of **C4**, and the spatial overlaps between these MOs are small. Due to the small spatial overlap between HOMO and LUMO, the DFT calculation may have a greater error than it did under normal condition. However, the DFT result supports the assumption that the 4-substituents of **C4** may have similar triplet energy level to the metal complex. Thus, the theory of reversible electronic energy transfer might be the explanation of the long photoluminescence lifetime of **C4**. DFT calculations of reference sample, lacking the methyl-groups on the 4-substituted phenyl groups, showed that different from **C4**, the LUMO (LUMO+1) and LUMO+2 are located around HOMO, thus, reversible electronic energy transfer may not happen on this kind of complex.

Compound	HOMO/ eV	LUMO/ eV	LUMO+1/ eV	LUMO+2/ eV	Eg/ eV
C1					3.61
	-5.04	-1.43	-1.40	-0.94	
C2					3.60
	-5.07	-1.47	-1.44	-1.00	
C3					3.59
	-5.06	-1.46	-1.43	-1.26	

Continued from previous sheet
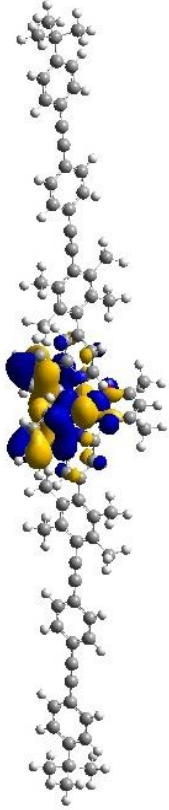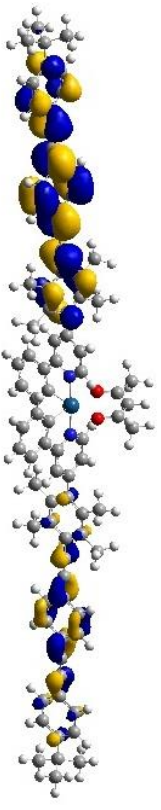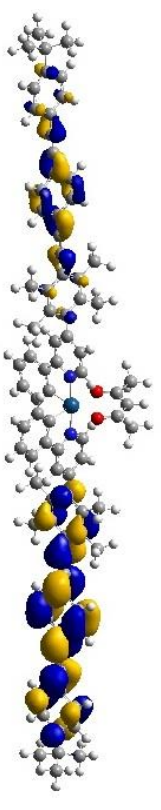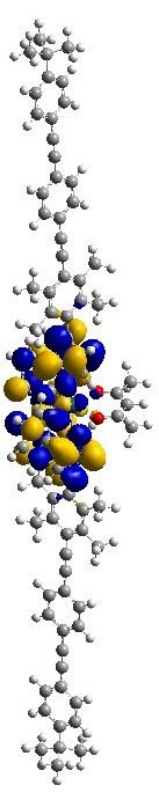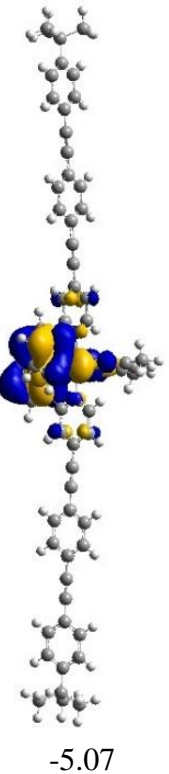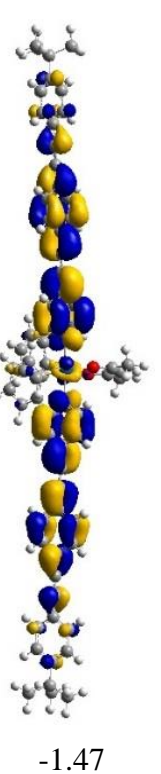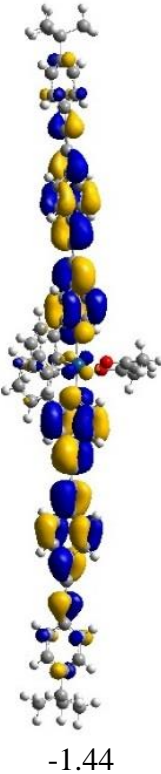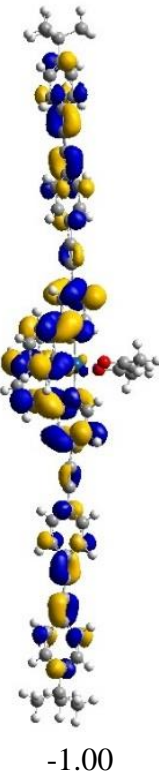
Compound	HOMO/ eV	LUMO/ eV	LUMO+1/ eV	LUMO+2/ eV	Eg/ eV
C4					3.61
	-5.04	-1.43	-1.40	-0.94	
sample without methyl groups at 4-substituted phenyl groups					3.60
	-5.07	-1.47	-1.44	-1.00	

Table *DFT results of target complexes **C1-4** and one similar sample*
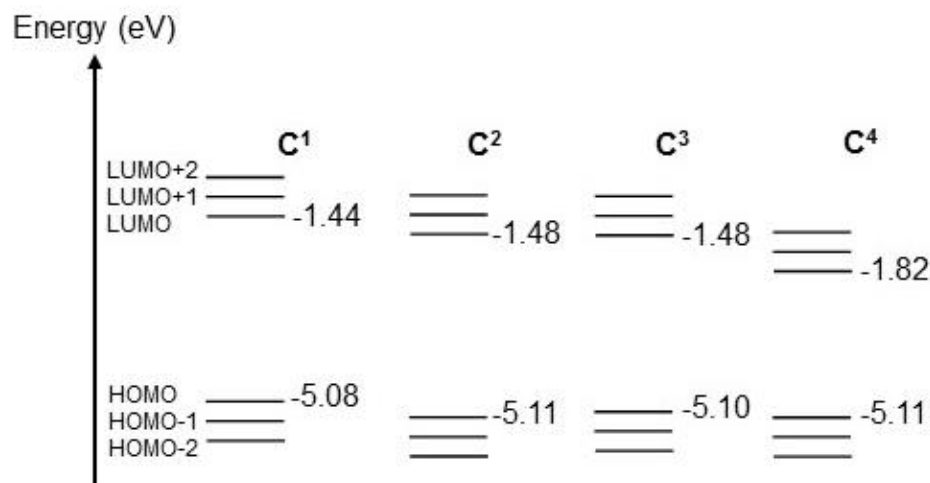
Figure 17 *Diagram indicating the energy levels of target complexes C1-4 as well as a rough*

comparison

3.4 Conclusion

In conclusion, absorption spectra, emission spectra, luminescence lifetime as well as PLQY of four related complexes have been measured. Comparing the absorption and emission spectra of **C1** with those of Ir(ppy)$_2$(acac) and Ir(dppy)$_3$ shows that by blocking the π-conjugation, **C1** gains the similar chemical structure as Ir(dppy)$_3$ without a significant red-shift. Furthermore, **C2**, **C3** and **C4** also have similar emission spectra as Ir(ppy)$_2$(acac) while changing the substituents. Based on experimental results, it has been proven that, by rotating the duryl bridge out of plane, cyclometalated iridium complexes with this kind of 4-substituted-2-phenyl-pyridine ligands are able to get rid of red-shift resulting from expansion of π-conjugation.

The enhanced PLQY of **C1** and **C2** have been observed, yet the mechanism remains covered. Meanwhile, an inference of the reason why **C3** and **C4** have relatively lower PLQY has been proposed indicating extra phenyl ethynyl groups may result in more significant non-radiative

decays. The luminescence lifetime of **C4** was found a lot longer than other complexes. However, the mechanism could only be proven with the aid of further photophysical studies.

DFT calculations, showed, that the *ortho*-methyl groups blocked the extension of π-conjugation. Thus, the MOs of these complexes and their energy levels of **C1-3** are similar to that of the parent complex, Ir(ppy)$_2$acac. The DFT calculations also supported the assumption that the long photoluminescence lifetime of **C4** may result from reversible electronic energy transfer between the central metal complex and the bis(phenylethynyl)benzene part of the ligands.

Chapter 4 Conclusion and future work

In order to understand the origin of **C4**'s long emission life time, the amount of twisting in the complex could be altered, *e.g.* reducing three or four methyl groups, making duryl into tolyl, phenyl, so that the steric hindrance would be reduced, as a result, the ring will be able to rotate. The assumption being that, by doing so, the conjugation and energy barrier between the substituents and pyridyl could be adjusted. In the main conjugated system, the electrons would be able to transfer from the iridium metal centre faster. That might lead to a shorter lifetime, therefore offering more evidence that a charge transfer process may be occurring. Another approach would be to add electron donating or withdrawing groups to the peripheral rings, or to add substituents with accessible triplet states from ^{3}MLCT to enhance a charge transfer mechanism. Varying the ancillary ligands would also be another via route for testing these complexes as they provide a convenient means of raising or lowering the energy levels of the metal centre. As shown in the **Figure 18**, a series of new complexes should be made and studied as comparison.
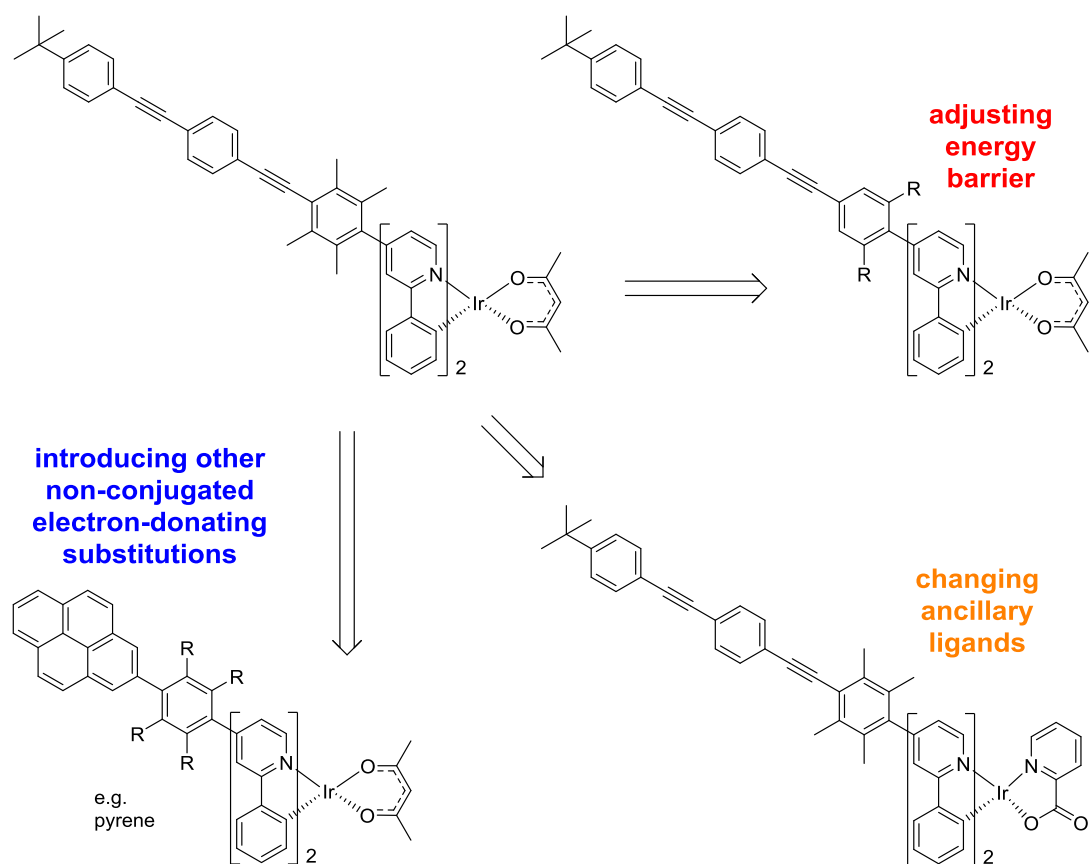
Figure 18 *Molecules should be studied in the future*

Furthermore, this kind of complexes which extended their length along one certain axis, do have unique steric configuration, compared to that of a complex which has similar length along all axes, with potential for orientation and polarised emission. As reported by Kim *et al.*, having a horizontal oriented transition dipole moment is related to the output efficiency of one OLED device. In this case, two conditions should be satisfied: (1) the molecule should have triplet transition dipole moments preferentially oriented along a specific direction and not have a combination of transition dipole moments with various orientations, and (2) the molecule itself should have a preferred orientation with respect to the substrate.[79] Based on this study, this kind of complex which in longer along one axis can be used to test its polarized emission. They should be trialled in an oriented film or material, and OLED to see

if aligning the molecules does give rise to polarized emission. Furthermore, with the technique of making hetero-leptic iridium complexes, molecules in **Figure 19** could be made. Thus, the transition dipole moments in the dye-doped co-host films could be further understood.
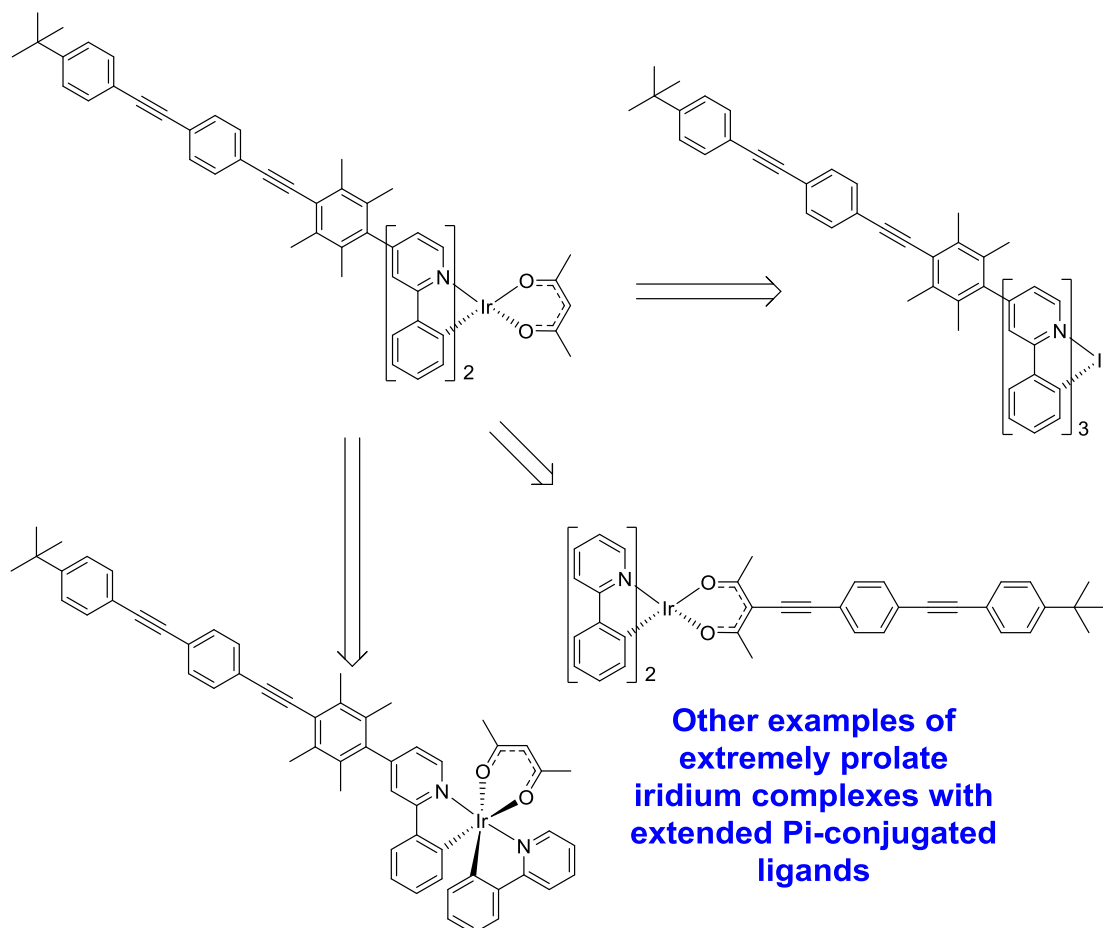
Figure 19 *Complexes that should be studied in the future in order to understand the horizontal oriented transition dipole moments in the dye-doped co-host films*

Chapter 5 Experimental procedures

5.1 Photophysics

All photophysical measurements were carried out with analytical grade solvents. Some of the iridium compounds can be photolytically degraded in chlorinated solvents, e.g. dichloromethane (DCM), as previously reported and observed in NMR spectroscopy.[80] Therefore, when using such solvents, samples were shielded from exposure to light and were only kept in solution for as short a time as possible. All diagrams are plotted with Microsoft Excel. The calculation of extinction coefficient, luminescence lifetimes (τ) and photoluminescence quantum yield (Φ_p) are done with Microsoft Excel.

5.1.1 UV-visible Absorption Spectroscopy

Absorption spectra were measured using quartz cuvettes with a pathlength, $l = 1$ cm, on a Unicam UV2-100 spectrometer operated with Unicam Vision software. A background reference spectrum of pure solvent was obtained for baseline correction. The Beer-Lambert law, $A = \varepsilon c l$ (c is concentration of the absorbing species, $mol \cdot dm^{-3}$, and l is the pathlength, cm) was used to calculate extinction coefficients ($\varepsilon, dm^3 \cdot mol^{-1} \cdot cm^{-1}$). Accurate concentrations were obtained by measuring sample masses on an analytical balance. Solutions were made up by using 1000 μL dropping pipette and volumetric flasks (5, 10, 50 and 100 mL).

5.1.2 Photoluminescence Spectroscopy

Excitation and emission photoluminescence spectra were recorded on a Horiba Jobin Yvon SPEX Fluorolog-3 spectrofluorometer using quartz cuvettes, $l = 1$ cm $\times$ 1 cm. Samples were

degassed by repeated freeze-pump-thaw cycles, typically to about 2.9×10^{-4} mbar, while being sealed with a Teflon Young's tap. PLQYs were measured using the integrating sphere technique,[81] with samples degassed as before. DataMax software was used during experiments.

5.1.3 Time Correlated Photon Counting (TCPC)

Luminescence lifetimes were measured using a TCPC technique. A pulsed nitrogen laser (337 nm, 1 ns pulse duration, 10 Hz repetition rate) was used to excite the sample, with a photomultiplier (Hamamatsu) to detect emitted photons and a National Instruments USB-5133 (8bit, 100 Ms/s) digitizer to acquire the data.

5.2 Density Functional Theory (DFT) Calculations

All calculations were undertaken by Dr Ross Davidson, and were performed with the Gaussian 09 program package,[82] using the B3LYP functional,[83, 84] the SDD basis set for all atoms and carried out in an dichloromethane solvent field using the SCRF-PCM method which creates the solvent cavity via a set of overlapping spheres.

5.3 Synthesis

All reagents were used as received without further purification and SPS dried solvents were used when anhydrous conditions were needed, De-ionised water was used where appropriate. Inert nitrogen atmosphere conditions were obtained using standard Schlenk-line apparatus and techniques. Column chromatography was performed on silica gel and monitored by thin layer chromatography (TLC) using fluorescent silica plates visualised under UV light. All synthesis was carried out in the Durham University Chemistry Department Lab CG100.

5.3.1 Analytical techniques

NMR spectra were obtained on a Bruker Avance-400, a Varian Inova-500 or a Varian VNMRS-700 instrument. Chemical shifts, δ, are reported in ppm and are internally referenced to the solvent residual peak. J coupling (^{1}H-^{1}H) values are reported in Hz. Where needed, the following 2D-NMR experiments were used to help assignment: ^{1}H-^{1}H Correlation Spectroscopy (COSY), Nuclear Overhauser Enhancement Spectroscopy (NOSEY), ^{1}H detected Heteronuclear Multiple Bond Correlation Spectroscopy (HMBC) and Heteronuclear Singular Quantum Correlation Spectroscopy (HSQC). Inequivalent protons are numbered sequentially as indicated in the chemical structures and are referred to as n-H, where n- is the proton number. Solvents used for NMR contains d-CHCl$_3$ and d$_2$-CH$_2$Cl$_2$. All NMR data were assigned and analysed using MestReNova.

Mass Spectrometry (MS) was performed with Gas Chromatography Mass Spectrometry (GC-MS), positive Electron Spray Ionisation (ESI+), Matrix Assisted-Laser Desorption Ionisation (MALDI) ToF and atmospheric pressure solids analysis probe ionisation (ASAP) by using Shimadzu QP2010-Ultra, TQD mass spectrometer, QtoF Premier mass spectrometer, LCT Premier XE mass spectrometer, Autoflex II ToF/ToF mass spectrometer (Bruker Daltonik GmBH) and Acquity UPLC (Waters Ltd, UK). Where a solvent was required, DCM was used expect for ESI+. DATA was collected by Mass Service Group of Department of Chemistry, Durham University.

Elemental analysis results were obtained using the elemental analysis service of London Metropolitan University, U.K. (Mr. S. Boyer).

Crystal structures were obtained by submitting to the Durham X-ray centre, with the results provided by Dr D.M.Yufit. The data were processed by using Mercury software.

5.3.2 Compound preparation

Intermediate **1** 4-4(-iodo-2,3,5,6-tetramethylphenyl)pyridine
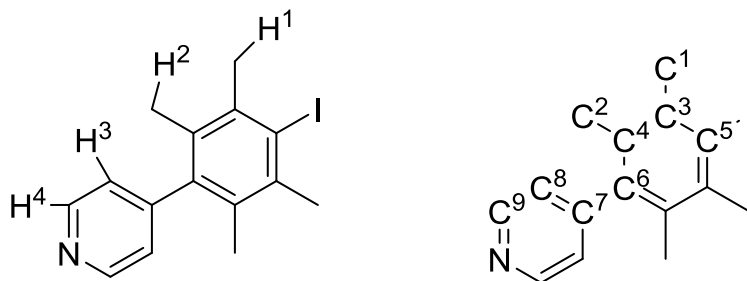
1,4-Diiodo-2,3,5,6-tetramethylbenzene (4.63 g, 12 mmol), 4-(4,4,5,5-tetramethyl-1,3,2-dioxaborolan-2-yl)-pyridine (820 mg, 4 mmol) and potassium carbonate (6.68 g, 48.3 mmol) were added into a two-necked round bottom flask. Then DMF (dried) (50 mL) was injected under N_2, followed by 3 degassing cylces, and stirred for approx. 5 min. Tetrakis (triphenylphosphine)palladium(0) (462 mg, 0.4 mmol) was added under a flow of N_2 and the mixture was heated at 90 °C under a nitrogen atmosphere for 12 hours with continuous stirring. The mixture was cooled to room temperature. Water (50 mL) was added and the mixture was extracted into dichloromethane (50 mL). The organic layer was washed with water (50 mL) in order to remove DMF and other inorganic materials. The mixture was dried over magnesium sulphate, filtered and evaporated to dryness. Column chromatography (silica gel/ 20 % ethyl acetate: hexane) afforded **1** as a clear white powder (450 mg, 44.5 %). ^{1}H NMR (700 MHz, Chloroform-*d*) δ H4 8.70 – 8.65 (m, 2H), H3 7.07 – 7.01 (m, 2H), H2 2.54 (s, 6H), H1 1.97 (s, 6H). ^{13}C NMR (176 MHz, Chloroform-*d*) δ C5 150.49 , C9 149.98 , C7 139.47 , C6 137.85 , C3 131.60 , C8 124.57 , C4 111.72 , C2 27.72 , C1 19.73 .HRMS (ES+): m/z 338.0394 [M+H]$^+$ (100%). Anal. Calc. for $C_{15}H_{16}NI$: C, 53.43; H, 4.78; N, 4.15 %. Found: C, 53.34; H, 4.70; N, 4.06 %.

Intermediate **2** 4-mesitylpyridine
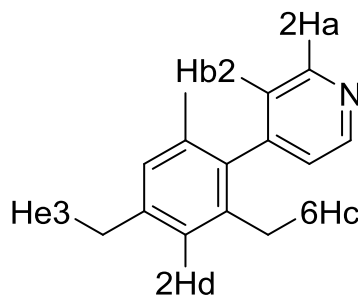
2,4,6-Trismethyliodobenzene (1.23 g, 5 mmol), 4-(4,4,5,5-tetramethyl-1,3,2-dioxaborolan-2-yl)-pyridine (820 mg, 4 mmol) and potassium carbonate (6.68 g, 48.3 mmol) were added into a two-necked round bottom flask. Then DMF (dried) (35 mL) was injected under N_2, followed with 3 cycles of degassing, and it was stirred for approx. 5 min. Tetrakis (triphenylphosphine)palladium(0) (462 mg, 0.4 mmol) was added under a flow of N_2. The mixture was heated at 90 ^{o}C under a nitrogen atmosphere for 12 hours with continuous stirring. The mixture was cooled to room temperature. Water (50 mL) was added and the mixture was extracted into dichloromethane (50 mL). The organic layer was washed with water (50 mL) in order to remove DMF and other inorganic materials. The mixture was dried over magnesium sulphate, filtered and evaporated to dryness. Column chromatography (silica gel/ 20 % ethyl acetate: hexane) afforded **2** as a clear white crystal like material (530 mg, 67.2 %). ^{1}H NMR (600 MHz, Chloroform-d) δ Ha 8.69 (d, 2H), Hb 7.16 – 7.01 (d, 2H), Hd 6.95 (s, 2H), He 2.33 (s, 3H), Hd 1.99 (s, 6H).

Intermediate **3** 1-bromo-4-iodo-2,3,5,6-tetramethylbenzene
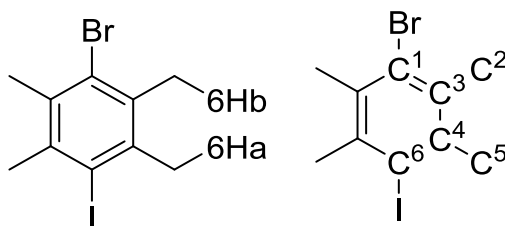
Bromodurene (5 g, 23.6 mmol), iodine (3.594 g, 14.16 mmol) and periodic acid (1.614 g, 7.08 mmol) were dissolved in a mixture of concentrated sulphuric acid (2.5 mL), water (12.5 mL) and glacial acetic acid (75 mL) in a two-necked round bottom flask. The mixture was heated at 40 °C for 12 hours with continuous stirring. Concentrated sodium thiosulfate solution (50 mL in water) was added and the mixture was extracted into dichloromethane (50 mL). The organic layer was washed with water (50 mL) in order to remove inorganic materials. The mixture was dried over magnesium sulphate, filtered and evaporated to dryness. Recrystallization of the crude material from acetone afforded **3** as white crystals (3.7 g, 46.25 %). ^{1}H NMR (700 MHz, Chloroform-*d*) δ Hb 2.58 (s, 6H), Ha 2.51 (s, 6H). ^{13}C NMR (176 MHz, Chloroform-*d*) δ C4 138.52 , C3 134.27 , C1 129.65 , C6 110.38 , C2 28.89 , C5 23.05 . HRMS (ES+): m/z 337.9177 [M]$^+$ (100%). Anal. Calc. for $C_{10}H_{12}BrI$: C, 35.43; H, 3.57. Found: C, 35.39; H, 3.43.

Intermediate **4** 4-mesityl-2-phenylpyridine
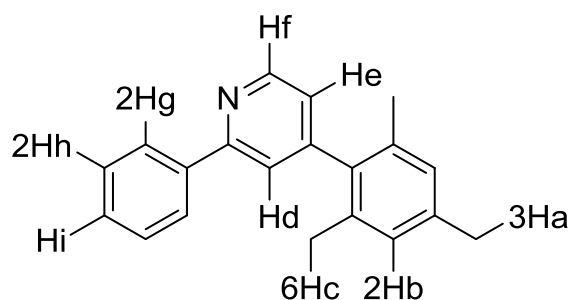
4-Mesitylpyridine (330 mg, 1.674 mmol) was dissolved with THF (25 mL) in a two-necked round bottom flask. Then it was cooled to -78 °C in (dry ice/ acetone) cooling bath, and it was stirred for approx. 5 min. Phenyl lithium (3.72 mL, 1.8 M in dibutyl ether, 6.696 mmol) was added in afterwards. The system was warmed to room temperature for 5 hours with continuous stirring after one hour. Water (50 mL) was added and the mixture was extracted

into dichloromethane (50 mL). The organic layer was washed with water (50 mL) in order to remove THF and other inorganic materials. The mixture was dried over magnesium sulphate, filtered and evaporated to dryness. The tough material was dissolved by diethyl ether (200 mL). Dried hydrogen chloride (diethyl ether solution 5 mL) was injected when stirring. Half of the solvent was removed by evaporation in order to precipitate the salt. The turbid liquid was filtered to get the sediment. The sediment was dissolved with methanol to remove other by-products. After that the salt was neutralised by additional diluted ammonium hydroxide (10%). Subsequence column chromatography (silica gel/ 20 % ethyl acetate: hexane) afforded **4** as a brown liquid (200 mg, 43.7 %). ^{1}H NMR (700 MHz, Chloroform-d) δ Hf 8.78 (dd, J = 4.8, 0.8 Hz, 1H), Hg 8.12 − 7.95 (m, 2H), Hd 7.66 − 7.56 (m, 1H), Hh 7.51 (dd, J = 8.4, 6.9 Hz, 2H), Hi 7.47 − 7.40 (m, 1H), He 7.09 (dd, J = 4.9, 1.6 Hz, 1H), Hb 7.02 (s, 2H), Ha 2.39 (s, 3H), Hc 2.09 (s, 6H).

Intermediate **5** 4-4(-bromo-2,3,5,6-tetramethylphenyl)pyridine
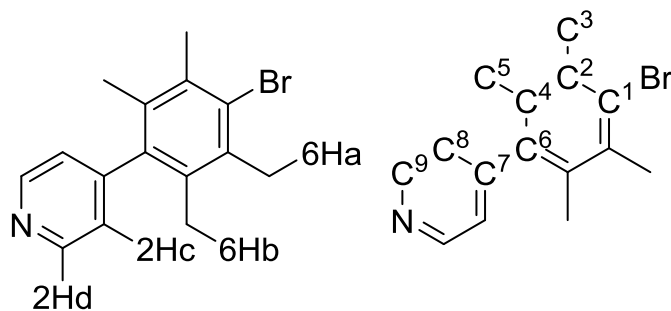
1-Bromo-4-iodo-2,3,5,6-tetramethylbenzene (813.6 mg, 2.4 mmol), 4-(4,4,5,5-tetramethyl-1,3,2-dioxaborolan-2-yl)-pyridine (410 mg, 2 mmol) and potassium carbonate (3.34 g, 24 mmol) were added into a two-necked round bottom flask. Then DMF (dried) (25 mL) was injected under N$_2$, followed 3 degassing cycles, and it was stirred for approx. 5 min. Tetrakis (triphenylphosphine)palladium(0) (231 mg, 0.2 mmol) was added under a flow of N$_2$. The mixture was heated at 90℃ under a nitrogen atmosphere for 12 hours with continuous stirring.

The mixture was cooled to room temperature. Water (50 mL) was added and the mixture was extracted into dichloromethane (50 mL). The organic layer was washed with water (50 mL) in order to remove DMF and other inorganic materials. The mixture was dried over magnesium sulphate, filtered and evaporated to dryness. Column chromatography (silica gel/ 20 % ethyl acetate: hexane) afforded **5** as brown crystals. ^{1}H NMR (700 MHz, Chloroform-d) δ 2Hd 8.70 – 8.61 (m, 2H), 2Hc 7.06 – 7.01 (m, 2H), 6Hb 2.44 (s, 6H), 6Ha 1.93 (s, 6H). ^{13}C NMR (176 MHz, Chloroform-*d*) δ C1 150.44 , C9 150.05 , C2 138.44 , C4 134.21 , C6 132.35 , C7 129.08 , C8 124.59 , C5 21.10 , C3 18.98 . HRMS (ES+): m/z 290.0537 [M+H]$^+$ (100%). Anal. Calc. for $C_{10}H_{12}BrI$: C, 62.08; H, 5.56; N, 4.83. Found: C, 62.04; H, 5.48; N, 5.02.

Intermediate **6** 4-(2,3,5,6-tetramethylphenyl)pyridine
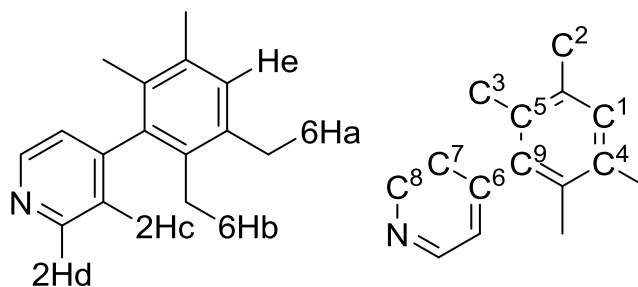
1-Bromo-2,3,5,6-tetramethylbenzene (529.6 mg, 2.5 mmol), 4-(4,4,5,5-tetramethyl-1,3,2-dioxaborolan-2-yl)-pyridine (410 mg, 2 mmol) and potassium carbonate (3.34 g, 24 mmol) were added into a two-necked round bottom flask. Then DMF (dried) (25 mL) was injected under N_2, followed by 3 degassing cycles, and it was stirred for approx. 5 min. Tetrakis (triphenylphosphine)palladium(0) (231 mg, 0.2 mmol) was added under a flow of N_2. The mixture was heated at 90 °C under a nitrogen atmosphere for 12 hours with continuous stirring. The mixture was cooled to room temperature. Water (50 mL) was added and the mixture was extracted into dichloromethane (50 mL). The organic layer was washed with

water (50 mL) in order to remove DMF and other inorganic materials. The mixture was dried over magnesium sulphate, filtered and evaporated to dryness. Column chromatography (silica gel/ 20 % ethyl acetate: hexane) afforded **6** as white crystals. ^{1}H NMR (600 MHz, Chloroform-d) δ 2Hd 8.69 – 8.63 (m, 2H), 2Hc 7.11 – 7.07 (m, 2H), He 7.03 (s, 1H), 6Ha 2.27 (s, 6H), 6Hb 1.87 (s, 6H). ^{13}C NMR (151 MHz, Chloroform-d) δ C6 150.97 , C7 149.79 , C9 139.27 , C5 133.88 , C1 131.14 , C5 130.99 , C8 124.84 , C2 20.06 , C3 17.06. Anal. Calc. for $C_{15}H_{17}N$: C, 85.26; H, 8.11; N, 6.63 %. Found: C, 85.14; H, 8.16; N, 6.74 %. HRMS (ES+): m/z 212.1433 $[M+H]^+$ (100%).

Intermediate **7** 4-(2,3,5,6-tetramethyl-[1,1'-biphenyl]-4-yl)pyridine
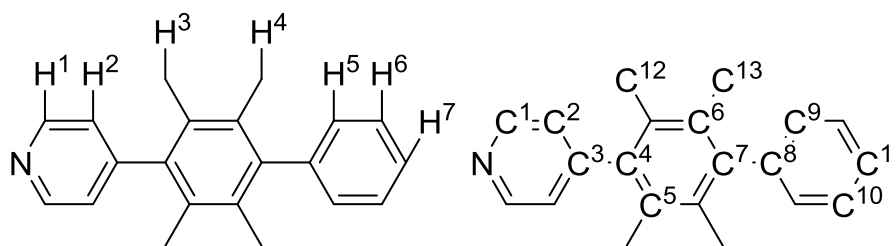
4-Iodo-2,3,5,6-tetramethyl-1,1'-biphenyl (1.11g, 3.83mmol) , 4-(4,4,5,5-tetramethyl-1,3,2-dioxaborolan-2-yl)pyridine (450 mg, 3.69 mmol) and potassium carbonate (4.5 g, 32.6 mmol) were added into a two-necked round bottom flask. Then DMF (dried) (50 mL) was injected under N_2, followed by 3 degassing cycles, and, stirred for approx. 5 min. Tetrakis (triphenylphosphine)palladium(0) (300 mg, 0.26 mmol) was added under a flow of N_2. The mixture was heated at 90 ℃ under a nitrogen atmosphere for 12 hours with continuous stirring. The mixture was cooled to room temperature. Water (50 mL) was added and the mixture was extracted into dichloromethane (50 mL). The organic layer was washed with water (50 mL) in order to remove DMF and other inorganic materials. The mixture was dried over magnesium sulphate, filtered and evaporated to dryness. Column chromatography (silica gel/ 20 % ethyl acetate: hexane) afforded **7** as a white powder (720 mg, 68 %). ^{1}H NMR (700

MHz, Chloroform-*d*) δ H1 8.68 (d, *J* = 5.3 Hz, 2H), H6 7.48 − 7.39 (m, 2H), H7 7.38 − 7.29 (m, 1H), H2 7.17 − 7.16 (m, 2H), H5 7.16 − 7.15 (m, 2H), H4 1.94 (s, 6H), H3 1.93 (s, 6H). ^{13}C NMR (176 MHz, Chloroform-*d*) δ C3 151.27 , C1 149.80 , C8 142.34 , C7 142.01 , C4 138.41 , C6 132.26 , C5 130.85 , C9 129.26 , C10 128.36 , C11 126.50 , C2 124.99 , C12/ C13 17.99 , C12/ C13 17.98 . HRMS (ES+): m/z 212.1433 [M+H]$^+$ (100%).

Ligand **1** 2-phenyl-4-(2,3,5,6-tetramethylphenyl)pyridine: **L1**

4-(2,3,5,6-Tetramethylphenyl)pyridine (1.2 g, 5.69 mmol) was dissolved with THF (40 mL) in a two-necked round bottom flask. Then it was cooled to -78 ℃ in (dry ice/ acetone) cooling bath. And it was stirred for approx. 5 min. Phenyl lithium (12 mL, 1.9 M in dibutyl ether, 22.76 mmol) was added in afterwards. The system was warmed to room temperature for 5 hours with continuous stirring after one hour. Water (100 mL) was added and the mixture was extracted into dichloromethane (100 mL)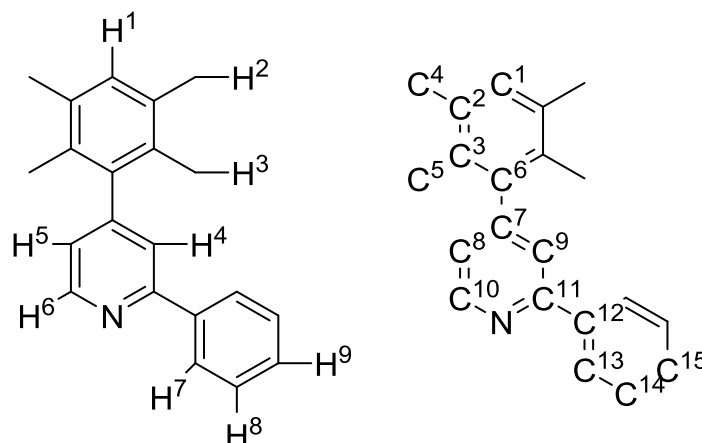. The organic layer was washed with water (100 mL) in order to remove THF and other inorganic materials. The mixture was dried over magnesium sulphate, filtered and evaporated to dryness. The crude material was dissolved in diethyl ether (200 mL). Dried hydrogen chloride in ether (5 mL) was injected with stirring. Half of the solvent was removed by evaporation in order to precipitate the salt. The turbid liquid was filtered to isolate the sediment. The sediment was dissolved in methanol to remove other by-products. After that the salt was neutralised by additional dilute ammonium hydroxide (10%). Column chromatography (silica gel/ 10 % ethyl acetate: hexane) afforded **L1** as light grey crystals (680 mg, 41.6 %). ^{1}H NMR (600 MHz, Chloroform-*d*) δ H6 8.74 (dd, *J* = 4.9, 0.9 Hz, 1H), H8 8.06 − 7.99 (m, 2H), H4 7.55 (dd, *J* = 1.5, 0.9 Hz, 1H), H7 7.50 − 7.44 (m, 2H), H9 7.44 − 7.39 (m, 1H), H1 7.05 (s, 1H), H5 7.04 (dd, *J* = 5.0, 1.5 Hz, 1H), H3

2.28 (s, 6H), H2 1.92 (s, 6H). ^{13}C NMR (151 MHz, Chloroform-d) δ C11 157.45 , C7 151.68 , C10 149.70 , C6 139.55 , C12 139.23 , C3 133.94 , C1 131.13 , C2 131.10 , C15 129.02 , C13 128.74 , C14 126.93 , C8 123.24 , C9 121.54 , C5 20.08 , C4 17.15 . HRMS (ES+): m/z 288.1749 [M+H]$^+$ (100%). Anal. Calc. for $C_{21}H_{21}N$: C, 87.76; H, 7.37; N, 4.87 %. Found: C, 87.60; H, 7.49; N, 4.87 %.

Complex **1** iridium(III) bis [2-phenyl-4-(2, 3, 5, 6-tetramethylphenyl) pyridinato-N, C2 ′] acetyl acetonate: **C1**
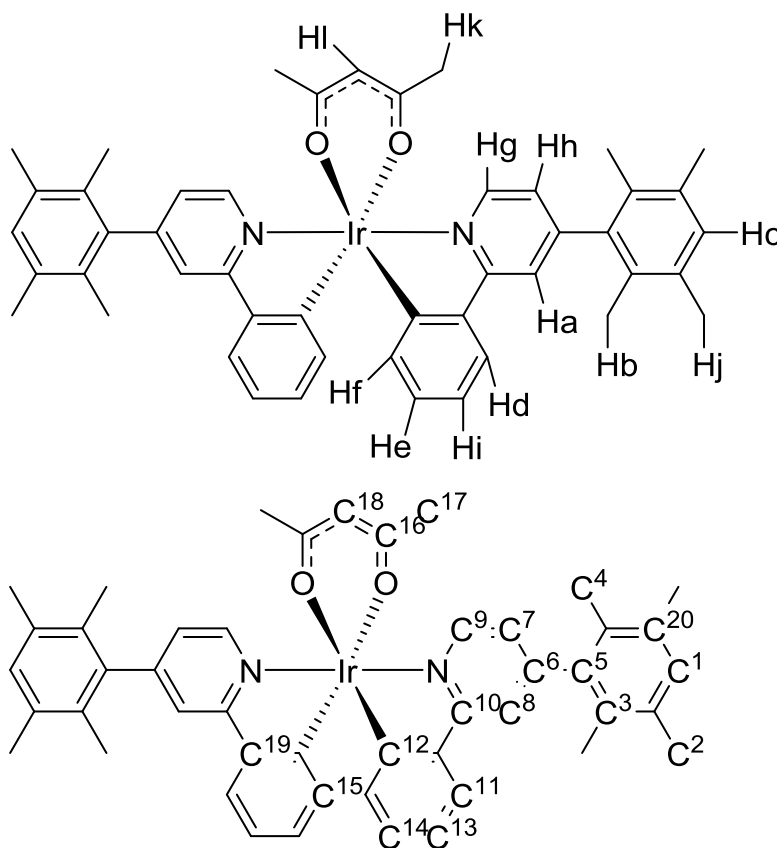
A mixture of **L1** (316 mg, 1.1 mmol), iridium(III) chloride trihydrate (176.3 mg, 0.5 mmol) were dissolved with 15 mL 2-ethoxyethanol and 5 mL water was heated under reflux for 25 h. The precipitated solid was separated by filtration, washed with water, purified with column

chromatography (silica gel/ 20 % ethyl acetate in dichloromethane) and dried to give the intermediate bis(μ-Cl)dimer (400mg). A mixture of this complex (400mg), acetyl acetone (1 mL), 2- ethoxyethanol (5 mL) and potassium carbonate (approx. 1 g) was heated under reflux overnight. Water was added to the cooled solution and the organic material extracted into dichloromethane. The extract was dried and evaporated to dryness and the product was purified by column chromatography (silica gel/ 20 % ethyl acetate in dichloromethane) afforded **C1** as a shiny dark green powder (330 mg, 34.5 %). ^{1}H NMR (700 MHz, Methylene Chloride-d_2) δ Hg 8.59 (dd, J = 5.6, 1.7 Hz, 2H), Ha 7.69 (d, J = 2.0 Hz, 2H), Hd 7.55 (dd, J = 7.8, 1.7 Hz, 2H), Hc 7.09 (s, 2H), Hh 7.03 (dd, J = 5.7, 1.9 Hz, 2H), Hi 6.86 (td, J = 7.3, 1.6 Hz, 2H), He 6.76 (td, J = 7.4, 1.7 Hz, 2H), Hf 6.41 (dd, J = 7.7, 1.7 Hz, 2H), Hl 5.38 (t, J = 1.5 Hz, 1H) Hj 2.32 (d, J = 9.0 Hz, 12H), Hb 2.06 (d, J = 46.0 Hz, 12H), Hk 1.88 (t, J = 1.5 Hz, 6H). ^{13}C NMR (176 MHz, Methylene Chloride-d_2) δ C16 184.74 , C12 168.12 , C10 152.31 , C9 147.94 , C6 147.45 , C19 145.35 , C5 138.95 , C20 133.97 (d, J = 8.7 Hz), C15 133.03 , C1 131.20 (d, J = 3.9 Hz), 131.10 , C14 128.79 , C11 123.86 , C7 123.25 , C13 120.74 , C8 119.87 , C18 100.42 , C17 28.36 , C2 19.82 (d, J = 7.0 Hz), C4 16.95 (d, J = 2.0 Hz). Anal. Calc. for $C_{47}H_{47}N_2O_2Ir$: C, 65.33; H, 5.48; N, 3.24 %. Found: C, 65.29; H, 5.33; N, 3.38 %. MS (MALDI TOF): m/z 864.4 [M]$^+$.

Intermediate **8** 4-(2,3,5,6-tetramethyl-4-((triisopropylsilyl)ethynyl)phenyl)pyridine
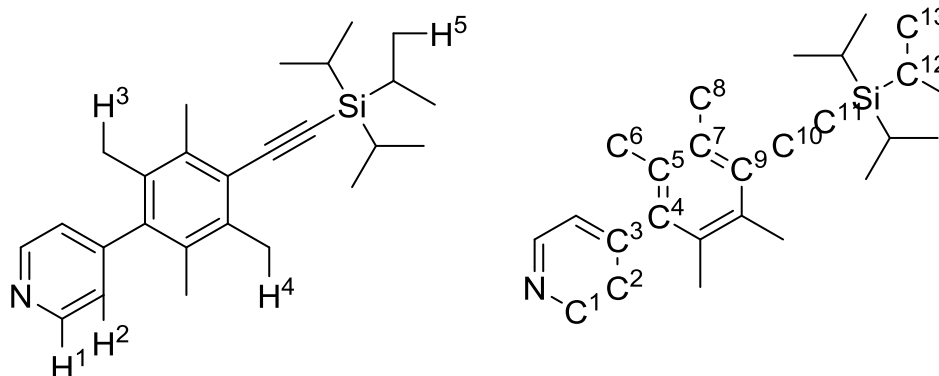
1 (1 g, 3 mmol), bis (tri phenyl phosphine) palladium(II) dichloride (290 mg, 0.4mmol) and copper iodide (85 mg, 0.4mmol) were added into a round bottom flask and degassed. 100 mL diisopropylamine (pre-distilled and degassed) was injected to the mixture, and degassed by 3 freeze-pump-thaw cycles, and the reaction mixture was stirred overnight at 50℃. The solvent was removed under reduced pressure and the residue purified by column chromatography (silica gel/ 20 % ethyl acetate in hexane) to afford **8** as light grey crystals. ^{1}H NMR (700 MHz, Chloroform-*d*) δ H1 8.67 (d, *J* = 4.8 Hz, 2H), H2 7.13 − 6.94 (m, 2H), H4 2.48 (s, 6H), H3 1.88 (s, 6H), H5 1.15 (d, *J* = 2.7 Hz, 21H). ^{13}C NMR (176 MHz, Chloroform-*d*) δ C3 150.79 , C1 149.87 , C4 139.24 , C7 136.61 , C5 130.85 , C2 124.63 , C9 123.80 , C10 105.33 , C11 99.04 , C13 18.72 , C8 18.50 , C6 17.80 , C12 11.37 . HRMS (ES+): m/z 392.2787 [M+H]$^+$ (100%). Anal. Calc. for $C_{26}H_{37}NSi$: C, 79.73; H, 9.52; N, 3.58 %. Found: C, 79.67; H, 9.50; N, 3.52 %.

Ligand **2** 2-phenyl-4-(2, 3, 5, 6-tetramethyl-4 ((tri isopropyl silyl) ethynyl) phenyl) pyridine:

L2
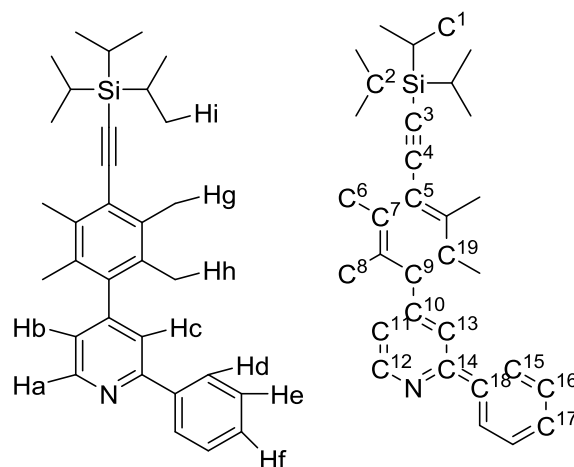
8 was dissolved with THF (100 mL) in a two-necked round bottom flask. Then it was cooled to -78℃ in (dry ice/ acetone) cooling bath, and it was stirred for approx. 5 min. Phenyl lithium (26.7 mL, 1.9 M in dibutyl ether, 50.64 mmol) was added in afterwards. The system was warmed to room temperature for 5 hours with continuous stirring after one hour. Methanol (100 mL) was added and the mixture was stirred for a while. 300 mg of activated charcoal was then added into the mixture. Solvents are removed by rotary evaporation. The mixture was dissolved by 300 mL of diethyl ether, and the precipitated solid was removed by filtration. Column chromatography (silica gel/ 5 % ethyl acetate: hexane) afforded **L2** as grey solid. (2.5g, 41.6%). ^{1}H NMR (700 MHz, Chloroform-*d*) δ Ha 8.74 (dd, *J* = 4.9, 0.9 Hz, 1H), He 8.11 − 7.93 (m, 2H), Hc 7.50 (t, *J* = 1.2 Hz, 1H), Hd 7.47 (t, *J* = 7.5 Hz, 2H), Hf 7.44 − 7.39 (m, 1H), Hb 7.00 (dd, *J* = 4.9, 1.5 Hz, 1H), Hh 2.50 (s, 6H), Hg 1.93 (s, 6H), Hi 1.16 (d, *J* = 2.6 Hz, 21H). ^{13}C NMR (151 MHz, Chloroform-*d*) δ C14 157.52 , C10 151.55 , C12 149.74 , C9 139.52 , C18 139.08 , C7 136.66 , C16 130.97 , C17 129.11 , C15 128.77 , C19 126.93 , C5 123.81 , C13 123.01 , C11 121.28 , C4 105.37 ,C3 99.03 , C1 18.72 , C6 18.53 ,

C8 17.89 , C2 11.38 . HRMS (ASAP): m/z 468.3085 [M+H]$^+$ (100%). Anal. Calc. for $C_{32}H_{41}NSi$: C, 82.17; H, 8.84; N, 2.99 %. Found: C, 81.99; H, 8.93; N, 3.22 %.

Complex **2** iridium(III) bis[2-phenyl-4-(2, 3, 5, 6-tetramethyl-4-((triisopropylsilyl)ethynyl) phenyl) pyridine) pyridinato-N, C2 ′] acetyl acetonate: **C2**
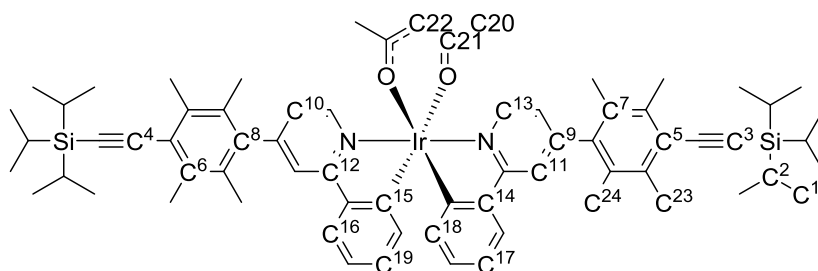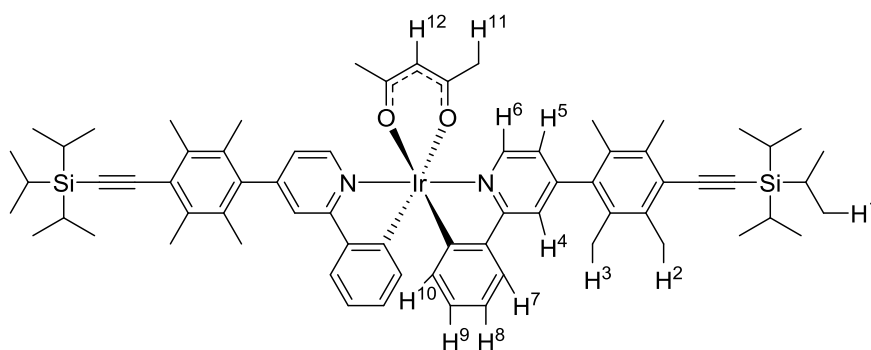
A mixture of **L2** (500 mg, 1.15 mmol), iridium(III) chloride trihydrate (150 mg,0.42mmol) were dissolved with 20 mL 2-ethoxyethanol and 10 mL water was heated under reflux for 25 h. The precipitated solid was separated by filtration, washed with water, purified with column chromatography (silica gel/ 20 % ethyl acetate in dichloromethane) and dried to give the intermediate bis(μ-Cl)dimer complex (400mg). A mixture of this complex (400mg), acetyl acetone (2 mL), 2- ethoxyethanol (5 mL) and potassium carbonate (approx. 1 g) was heated under reflux overnight. The organic ingredient was separated by extraction (water/ dichloromethane) and evaporated to dryness and the product was purified by column

chromatography (silica gel/ 20 % ethyl acetate in dichloromethane) afforded **C2** as a shiny yellow powder (340 mg, 27 %).^{1}H NMR (700 MHz, Methylene Chloride-d_2) δ 8.58 (dd, J = 5.7, 0.7 Hz, 2H), 7.67 − 7.64 (m, 2H), 7.54 (dd, J = 7.8, 1.4 Hz, 2H), 7.00 (dd, J = 5.7, 1.8 Hz, 2H), 6.86 (td, J = 7.4, 1.3 Hz, 2H), 6.76 (td, J = 7.4, 1.4 Hz, 2H), 6.39 (dd, J = 7.7, 1.2 Hz, 2H), 2.55 (d, J = 9.5 Hz, 12H), 2.11 (s, 6H), 1.87 (s, 6H), 1.20 (d, J = 3.1 Hz, 42H). ^{13}C NMR (176 MHz, Methylene Chloride-d_2) δ C21 184.78 , C15 168.20 , C12 152.01 , C13 148.01 , C9 147.47 , C14 145.22 , C8 139.01 , C7 136.67 (d, J = 8.1 Hz), C18 133.01 , C6 131.12 (d, J = 14.4 Hz), C19 128.87 , C16 123.92 , C5 123.79 , C10 123.02 , C17 120.78 , C11 119.61 , C4 105.48 , C22 100.43 , C3 99.04 , C20 28.34, C1 18.51 , C24 18.34 (d, J = 6.6 Hz), C23 17.72 (d, J = 2.3 Hz), C2 11.40 . MS (MALDI): m/z 1224.5 [M]$^+$. Anal. Calc. for $C_{69}H_{87}N_2O_2Si_2Ir$: C, 67.66; H, 7.16; N, 2.29 %. Found: C, 67.49; H, 6.93; N, 2.36 %

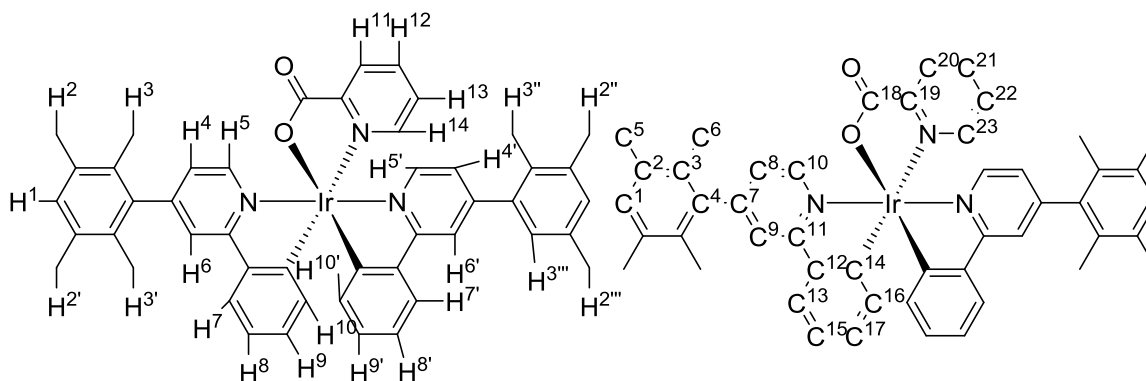Complex **5** iridium(III) bis [2-phenyl-4-(2, 3, 5, 6-tetramethyl-4-((triisopropylsilyl)ethynyl) phenyl)pyridine) pyridinato-N, C2 ′] picolinate: **C5**

A mixture of **L1** (500 mg, 1.74 mmol), iridium(III) chloride trihydrate(207 mg,0.53mmol) were dissolved with 20 mL 2-ethoxyethanol and 10 mL water was heated under reflux for 25 h. The precipitated solid was separated by filtration, washed with water, purified with column chromatography (silica gel/ 20 % ethyl acetate in dichloromethane) and dried to give the intermediate bis(μ-Cl)dimer complex (400mg). A mixture of this complex (400mg), 2-

picolinic acid (approx. 160mg), 2- ethoxyethanol (5 mL) and potassium carbonate (approx. 1 g) was heated under reflux overnight. The organic ingredient was separated by extraction (water/ dichloromethane) and evaporated to dryness and the product was purified by column chromatography (silica gel/ 20 % ethyl acetate in dichloromethane) afforded C5 as a shiny yellow powder (350 mg, 25 %).^{1}H NMR (700 MHz, Methylene Chloride-d_2) δ 8.80 (d, J = 5.9 Hz, 1H), 8.33 (d, J = 7.9 Hz, 1H), 7.95 (tt, J = 7.7, 1.5 Hz, 1H), 7.93 – 7.88 (m, 1H), 7.75 (d, J = 1.9 Hz, 1H), 7.69 (d, J = 1.8 Hz, 1H), 7.62 (t, J = 7.8 Hz, 2H), 7.57 (d, J = 5.8 Hz, 1H), 7.40 (ddd, J = 7.3, 5.4, 1.4 Hz, 1H), 7.06 (d, J = 2.3 Hz, 2H), 7.01 (dd, J = 5.8, 1.7 Hz, 1H), 6.98 – 6.90 (m, 2H), 6.87 (ddd, J = 13.6, 8.1, 6.8 Hz, 2H), 6.82 (dd, J = 5.9, 1.8 Hz, 1H), 6.50 (d, J = 7.6 Hz, 1H), 6.36 (d, J = 7.6 Hz, 1H), 2.30 (d, J = 5.1 Hz, 6H), 2.29 (s, 3H), 2.26 (s, 3H), 2.06 (s, 3H), 2.03 (s, 3H), 2.00 (s, 3H), 1.84 (s, 3H).

Intermediate **9** 4-iodo-2,3,5,6-tetramethyl-1,1'-biphenyl
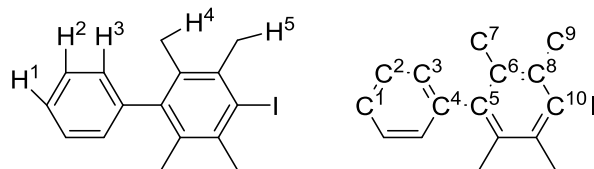
1,4-Diiodo-2,3,5,6-tetramethylbenzene (17.8 g, 46 mmol), phenyl boronic acid (1.86 g, 15.3 mmol) and potassium carbonate (25 g, 4 equiv.) were added into a two-necked round bottom flask. Then DMF (dried) (200 mL) was injected under N_2, followed with 3 times of degas, and stirred for approx. 5 min. Ttrakis(triphenylphosphine)palladium(0) (1.77 g, 1.53 mmol) was added under a flow of N_2. The mixture was heated at 90℃ under a nitrogen atmosphere for 12 hours with continuous stirring. The mixture was cooled to room temperature. Water (200 mL) was added and the mixture was extracted into dichloromethane (2000 mL). The organic layer was washed with water (50 mL) in order to remove DMF and other inorganic materials. The mixture was dried over magnesium sulphate, filtered and evaporated to

dryness. Column chromatography (silica gel/ 20 % ethyl acetate: hexane) afforded **9** as a white powder (1.8 g, 35 %). ^{1}H NMR (700 MHz, Chloroform-*d*) δ H2 7.43 − 7.37 (m, 2H), H1 7.33 (ddt, *J* = 8.0, 6.9, 1.3 Hz, 1H), H3 7.09 − 7.05 (m, 2H), H4 2.55 (s, 6H), H5 1.99 (s, 6H). ^{13}C NMR (176 MHz, Chloroform-*d*) δ C4/ C5 142.26 , C4/ C5 142.02 , C8 137.35 , C6 132.73 , C3 129.09 , C2 128.40 , C1 126.58 , C10 110.87 , C7 27.78 , C9 19.85 . HRMS (ES+): m/z 336.0374 [M]$^+$ (100%).

Intermediate **10** 1-(tert-butyl)-4-((4-iodophenyl)ethynyl)benzene
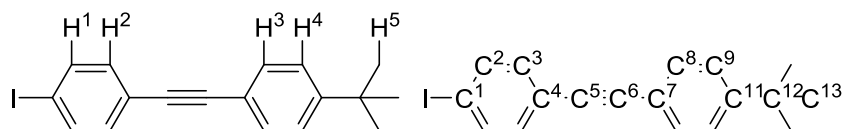
1-(Tert-butyl)-4-((4-bromophenyl)ethynyl)benzene(3.15 g, 10 mmol), was dissolved in THF in a two-necked round bottom flask which was then cooled to -78 ℃. *n*-Butyl lithium(2.5 M in Hexane, 4 mL, 10 mmol) was dropwise injected. Iodine(4 g, excessive) THF mixture was injected after the reaction was stirred for approx. 15 min. Reaction was slowly warmed to room temperature afterwards while continuously stirring, and it was reacted for another 4 hours. Solvent was removed by rotary evaporators. Aqueous sodium thiosulfate was added in order to remove excess iodine. And was dried by Magnesium sulphate and columned with silca gel/ hexane to obtain pure white powder(2.5 g, 70%). ^{1}H NMR (700 MHz, Chloroform-d) δ H1/ H2/ H3/ H4 7.51 − 7.42 (m, 4H), H1/ H2/ H3/ H4 7.41 − 7.32 (m, 4H), H5 1.32 (s, 9H). ^{13}C NMR (176 MHz, Chloroform-d) δ C11 151.81 , C2/ C3/ C8/ C9 132.96 , C2/ C3/ C8/ C9 131.53 , C2/ C3/ C8/ C9 131.29 , C2/ C3/ C8/ C9 125.38 , C1/ C4/ C7 122.47 , C1/ C4/ C7 122.20 , C1/ C4/ C7 119.84 , C6 90.66 , C5 87.64 , C12 34.80 , C13 31.14 . HRMS (ASAP): m/z 360.0372 [M]+ (100%). Anal. Calc. for C18H17I: C, 60.02; H, 4.76. Found: C, 59.95; H, 4.68%.

Complex **4** iridium(III) bis[4-(4-((4-((4-(tert-butyl)phenyl)ethynyl)phenyl)ethynyl)-2,3,5,6-tetramethyl phenyl)-2-phenylpyridine) pyridinato-N, C2 '] acetyl acetonate: **C4**
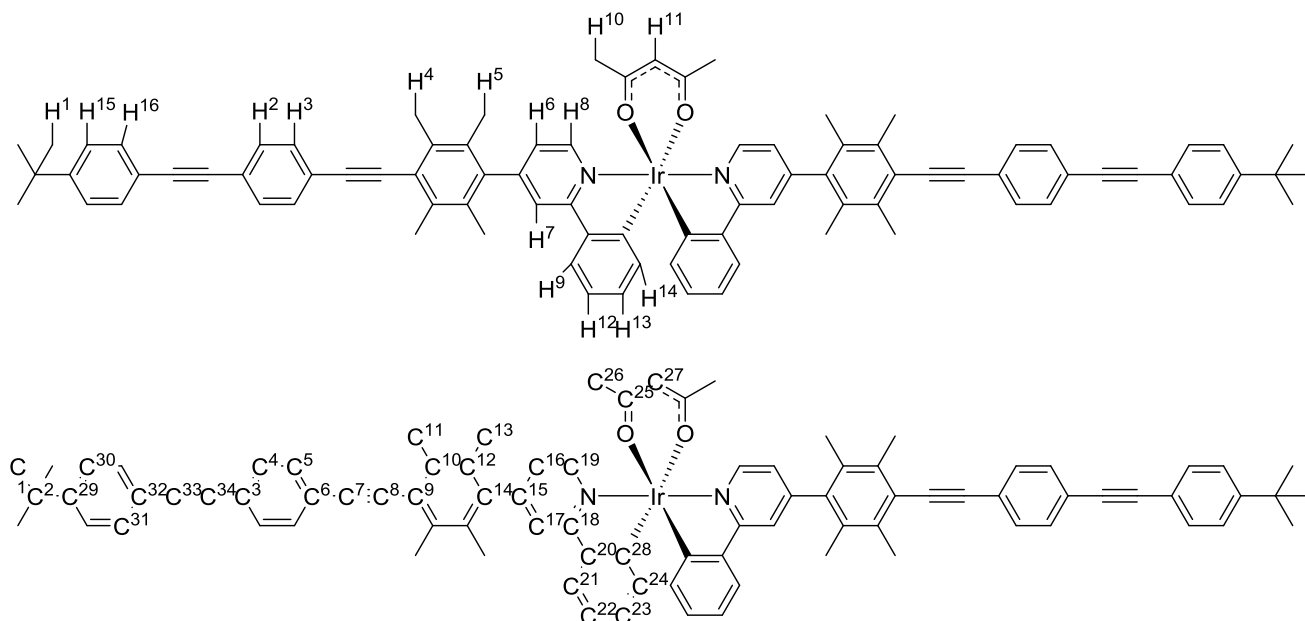
C2 (300 mg, 0.24 mmol), bis(triphenyl phosphine) palladium(II) dichloride (17 mg, 0.024mmol), **10**(180mg, 0.5 mmol) and copper iodide (4 mg, <0.02mmol) were added into a two-neck round bottom flask and degassed. 25 mL THF (pre-distilled and degassed) and 25ml Et$_3$N was injected, and the mixture was degassed by 3 times of freeze-pump-thaws. Tetrabutylammonium fluoride (1 M solution in THF, 0.48 mL, 0.48 mmol) was added, and the reaction mixture was stirred overnight at 50℃.Evaporate solvent from the mixture, Column chromatography (silica gel/ dichloromethane) afforded **C4** as a brown crystal.

^{1}H NMR (700 MHz, Methylene Chloride-d_2) δ H8 8.64 − 8.57 (m, 2H), H15, H16/ H2, H3 7.70 − 7.69 (m, 4H), H15, H16/ H2, H3 7.61 − 7.59 (m, 4H), H14 7.58 − 7.55 (m, 2H), H15, H16/ H2, H3 7.50 (dq, J = 8.3, 1.9 Hz, 4H), H15, H16/ H2, H3 7.45 − 7.42 (m, 4H), H7 7.30 − 7.25 (m, 2H), H6 7.04 (dd, J = 5.7, 1.9 Hz, 2H), H13 6.87 (td, J = 7.4, 1.3 Hz, 2H), H12 6.77 (ddd, J = 8.1, 7.1, 1.4 Hz, 2H), H9 6.41 (dd, J = 7.7, 1.2 Hz, 2H), H11 5.38 (s, 1H), H4/

H5 2.61 (s, 6H), H4/ H5 2.59 (s, 6H), H4/ H5 2.15 (s, 6H), H4/ H5 2.08 (s, 6H), H10 1.88 (s, 6H), H1 1.35 (s, 18H). MS (MALDI TOF): m/z 1376.4 [M]$^+$ (100%). Anal. Calc. for C$_{87}$H$_{79}$N$_2$O$_2$Ir+ CH$_2$Cl$_2$: C, 72.31; H, 5.59; N, 1.92%. Found: C, 72.31; H, 5.78; N, 1.92%.

Complex **3** iridium(III) bis [4-(4-((4-(tert-butyl)phenyl)ethynyl)-2,3,5,6-tetramethylphenyl)-2-phenyl pyridine) pyridinato-N, C2 '] acetyl acetonate: **C3**
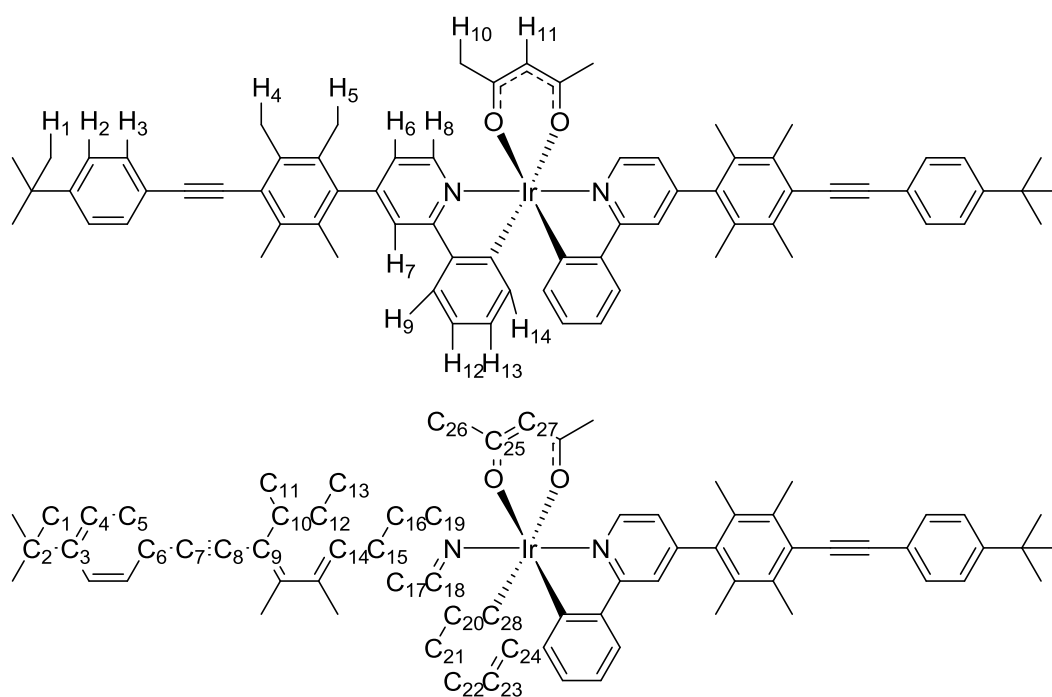
C2 (300 mg, 0.24 mmol), bis(triphenyl phosphine) palladium(II) dichloride (17 mg, 0.024mmol), 1-(tert-butyl)-4-iodobenzene (130mg, 0.5 mmol) and copper iodide (4 mg, <0.02mmol) were added into a two-neck round bottom flask and degassed. 25 mL THF (pre-distilled and degassed) and 25ml Et$_3$N was injected, and the mixture was degassed by 3 times of freeze-pump-thaws. Tetrabutylammonium fluoride (1 M solution in THF, 0.48 mL, 0.48 mmol) was added, and the reaction mixture was stirred overnight at 50℃.Evaporate solvent

from the mixture, Column chromatography (silica gel/ dichloromethane) afforded **C3** as a brown crystal.

^{1}H NMR (700 MHz, Methylene Chloride-d_2) δ H8 8.62 – 8.54 (m, 2H), H7 7.69 (d, J = 1.8 Hz, 2H), H9& H2/ H3 7.58 – 7.51 (m, 6H), H2/ H3 7.46 – 7.42 (m, 4H), H6 7.03 (dd, J = 5.7, 1.8 Hz, 2H), H12 6.86 (td, J = 7.4, 1.2 Hz, 2H), H13 6.80 – 6.73 (m, 2H), H10 6.40 (dd, J = 7.7, 1.2 Hz, 2H), H11 5.37 (s, 1H), H5 2.59 (s, 6H), H5' 2.58 (s, 6H), H4 2.14 (s, 6H), H4' 2.07 (s, 6H), H10 1.88 (s, 6H), H1 1.36 (s, 21H). ^{13}C NMR (176 MHz, Methylene Chloride-d_2) δ C25 184.78 , C28 168.20 , C18 152.05 , C6/ C9 151.61 , C19 148.01 , C15 147.48 , C20 145.25 , C14 138.95 , C17 136.21 , C24 136.16 , C10 133.02 , C23 131.26 , C21 131.18 , C12 130.94 , C16 128.86 , C19 125.43 , C22 123.93 , C6/ C9 123.51 , C4/ C5 123.06 , C4/ C5 120.78 , C3 120.67 , C27 119.67 , 100.43 , C7/ C8 97.51 , C7/ C8 87.59 , C2 34.67 , C1 30.88 , C26 28.36 , C11/ C13 18.29 , C11/ C1318.26 , C11/ C13 17.77 , C11/ C13 17.76 . HRMS (ASAP): m/z 1176.5151 [M]$^+$ (100%). Anal. Calc. for $C_{71}H_{71}N_2O_2Ir$: C, 72.48; H, 6.08; N, 2.38%. Found: C, 72.62; H, 5.93; N, 1.92%.

Reference list

1.   S. R. Forrest, *Organic Electronics*, 2003, **4**, 45-48.
2.   F.-M. Tseng, A.-C. Cheng and Y.-N. Peng, *Technological Forecasting and Social Change*, 2009, **76**, 897-909.
3.   T.-H. Liu, C.-Y. Iou and C. H. Chen, *Applied Physics Letters*, 2003, **83**, 5241-5243.
4.   M. Pfeiffer, S. R. Forrest, K. Leo and M. E. Thompson, *Advanced Materials*, 2002, **14**, 1633-1636.
5.   Q. Pei, G. Yu, C. Zhang, Y. Yang and A. J. Heeger, *Science*, 1995, **269**, 1086-1088.
6.   C.-C. Chang, J.-Y. Wu, C.-W. Chien, W.-S. Wu, H. Liu, C.-C. Kang, L.-J. Yu and T.-C. Chang, *Analytical Chemistry*, 2003, **75**, 6177-6183.
7.   S. Tao, Z. Peng, X. Zhang, P. Wang, C. S. Lee and S. T. Lee, *Advanced Functional Materials*, 2005, **15**, 1716-1721.
8.   B. Schade, V. Hagen, R. Schmidt, R. Herbrich, E. Krause, T. Eckardt and J. Bendig, *The Journal of Organic Chemistry*, 1999, **64**, 9109-9117.
9.   M. A. Baldo, D. O'brien, Y. You, A. Shoustikov, S. Sibley, M. Thompson and S. Forrest, *Nature*, 1998, **395**, 151-154.
z10.   M. G. Colombo, T. C. Brunold, T. Riedener, H. U. Guedel, M. Fortsch and H.-B. Bürgi, *Inorganic Chemistry*, 1994, **33**, 545-550.
11.   S. Lamansky, P. Djurovich, D. Murphy, F. Abdel-Razzaq, H.-E. Lee, C. Adachi, P. E. Burrows, S. R. Forrest and M. E. Thompson, *Journal of the American Chemical Society*, 2001, **123**, 4304-4312.
12.   T. Tsuzuki, N. Shirasawa, T. Suzuki and S. Tokito, *Advanced Materials*, 2003, **15**, 1455-1458.
13.   P. J. Hay, *The Journal of Physical Chemistry A*, 2002, **106**, 1634-1641.
14.   M. Baldo, S. Lamansky, P. Burrows, M. Thompson and S. Forrest, *Applied Physics Letters*, 1999, **75**, 4.
15.   A. Beeby, S. Bettington, I. D. Samuel and Z. Wang, *Journal of Materials Chemistry*, 2003, **13**, 80-83.
16.   A. Endo, K. Suzuki, T. Yoshihara, S. Tobita, M. Yahiro and C. Adachi, *Chemical Physics Letters*, 2008, **460**, 155-157.
17.   S. Lamansky, P. Djurovich, D. Murphy, F. Abdel-Razzaq, R. Kwong, I. Tsyba, M. Bortz, B. Mui, R. Bau and M. E. Thompson, *Inorganic Chemistry*, 2001, **40**, 1704-1711.
18.   V. N. Kozhevnikov, Y. Zheng, M. Clough, H. A. Al-Attar, G. C. Griffiths, K. Abdullah, S. Raisys, V. Jankus, M. R. Bryce and A. P. Monkman, *Chemistry of Materials*, 2013, **25**, 2352-2358.
19.   H. Yersin, in *Transition Metal and Rare Earth Compounds*, Springer, Editon edn., 2004, pp. 1-26.
20.   R. Friend, R. Gymer, A. Holmes, J. Burroughes, R. Marks, C. Taliani, D. Bradley, D. Dos Santos, J. Bredas and M. Lögdlund, *Nature*, 1999, **397**, 121-128.
21.   C. W. Tang and S. A. VanSlyke, *Applied Physics Letters*, 1987, **51**, 913-915.
22.   H. Aziz, Z. D. Popovic, N.-X. Hu, A.-M. Hor and G. Xu, *Science*, 1999, **283**, 1900-1902.
23.   J. Kido and Y. Okamoto, *Chemical Reviews*, 2002, **102**, 2357-2368.
24.   V.-E. Choong, S. Shi, J. Curless, C.-L. Shieh, H.-C. Lee, F. So, J. Shen and J. Yang, *Applied Physics Letters*, 1999, **75**, 172-174.
25.   D. Zhang, K. Ryu, X. Liu, E. Polikarpov, J. Ly, M. E. Tompson and C. Zhou, *Nano Letters*, 2006, **6**, 1880-1886.

26.   C. Adachi, M. A. Baldo, S. R. Forrest and M. E. Thompson, *Applied Physics Letters*, 2000, **77**, 904.

27.   Y. Shirota and H. Kageyama, *Chemical Reviews*, 2007, **107**, 953-1010.

28.   H. Mattoussi, H. Murata, C. D. Merritt, Y. Iizumi, J. Kido and Z. H. Kafafi, *Journal of Applied Physics*, 1999, **86**, 2642-2650.

29.   C. Adachi, R. C. Kwong, P. Djurovich, V. Adamovich, M. A. Baldo, M. E. Thompson and S. R. Forrest, *Applied Physics Letters*, 2001, **79**, 2082-2084.

30.   J. J. Lin, W. S. Liao, H. J. Huang, F. I. Wu and C. H. Cheng, *Advanced Functional Materials*, 2008, **18**, 485-491.

31.   C. Adachi, M. A. Baldo, M. E. Thompson and S. R. Forrest, *Journal of Applied Physics*, 2001, **90**, 5048-5051.

32.   B. X. Mi, P. F. Wang, Z. Q. Gao, C. S. Lee, S. T. Lee, H. L. Hong, X. M. Chen, M. S. Wong, P. F. Xia and K. W. Cheah, *Advanced Materials*, 2009, **21**.

33.   T. Tsuzuki and S. Tokito, *Advanced Materials*, 2007, **19**, 276-280.

34.   L. Shi, J. Su and Z. Wu, *Inorganic Chemistry*, 2011, **50**, 5477-5484.

35.   K. Okinaka, A. Saitoh, N. Yamada, M. Yashima, K. Suzuki, A. Senoo and K. Ueno, Google Patents, Editon edn., 2009.

36.   J. Shi and C. W. Tang, *Applied Physics Letters*, 2002, **80**, 3201-3203.

37.   T. Yu, P. Zhang, Y. Zhao, H. Zhang, J. Meng and D. Fan, *Organic Electronics*, 2009, **10**, 653-660.

38.   L. Picciolo, H. Murata and Z. Kafafi, *Applied Physics Letters*, 2001.

39.   Y. Ohmori, H. Kajii, T. Sawatani, H. Ueta and K. Yoshino, *Thin Solid Films*, 2001, **393**, 407-411.

40.   K. Dedeian, J. Shi, N. Shepherd, E. Forsythe and D. C. Morton, *Inorganic Chemistry*, 2005, **44**, 4445-4447.

41.   E. Baranoff, J.-H. Yum, M. Graetzel and M. K. Nazeeruddin, *Journal of Organometallic Chemistry*, 2009, **694**, 2661-2670.

42.   M. Nonoyama, *Bulletin of the Chemical Society of Japan*, 1974, **47**, 767-768.

43.   A. Suzuki, *Journal of Organometallic Chemistry*, 1999, **576**, 147-168.

44.   J. K. Stille, *Angewandte Chemie International Edition in English*, 1986, **25**, 508-524.

45.   C. Wolf and B. T. Ghebremariam, *Synthesis*, 2002, 749-752.

46.   E.-I. Negishi and T. Takahashi, *Accounts of Chemical Research*, 1994, **27**, 124-130.

47.   E.-I. Negishi, F.-T. Luo, R. Frisbee and H. Matsushita, *Heterocycles*, 1982, **18**, 117-122.

48.   S. Çalimsiz, M. Sayah, D. Mallik and M. G. Organ, *Angewandte Chemie International Edition*, 2010, **49**, 2014-2017.

49.   R. M. Edkins, S. L. Bettington, A. E. Goeta and A. Beeby, *Dalton Transactions*, 2011, **40**, 12765-12770.

50.   F. Kröhnke, *Angewandte Chemie International Edition in English*, 1963, **2**, 380-393.

51.   R. Karki, P. Thapa, M. J. Kang, T. C. Jeong, J. M. Nam, H.-L. Kim, Y. Na, W.-J. Cho, Y. Kwon and E.-S. Lee, *Bioorganic & Medicinal Chemistry*, 2010, **18**, 3066-3077.

52.   K. King, P. Spellane and R. J. Watts, *Journal of the American Chemical Society*, 1985, **107**, 1431-1432.

53.   Y. You and S. Y. Park, *Dalton Transactions*, 2009, 1267-1282.

54.   H. Sun, S. Liu, W. Lin, K. Y. Zhang, W. Lv, X. Huang, F. Huo, H. Yang, G. Jenkins and Q. Zhao, *Nature Communications*, 2014, **5**.

55.   Q. Zhao, F. Li, S. Liu, M. Yu, Z. Liu, T. Yi and C. Huang, *Inorganic chemistry*, 2008, **47**, 9256-9264.

56.   J. W. Lichtman and J.-A. Conchello, *Nature Methods*, 2005, **2**, 910-919.

57.   C. Tang, S. VanSlyke and C. Chen, *Journal of Applied Physics*, 1989, **65**, 3610-3616.

58.   S.-y. Takizawa, H. Echizen, J.-i. Nishida, T. Tsuzuki, S. Tokito and Y. Yamashita, *Chemistry Letters*, 2006, **35**, 748-749.

59.   K. Dedeian, P. Djurovich, F. Garces, G. Carlson and R. Watts, *Inorganic Chemistry*, 1991, **30**, 1685-1687.

60.   S. Jung, Y. Kang, H. S. Kim, Y. H. Kim, C. L. Lee, J. J. Kim, S. K. Lee and S. K. Kwon, *European Journal of Inorganic Chemistry*, 2004, **2004**, 3415-3423.

61.   J. Roncali, *Chemical Reviews*, 1997, **97**, 173-206.

62.   A. Tsuboyama, H. Iwawaki, M. Furugori, T. Mukaide, J. Kamatani, S. Igawa, T. Moriyama, S. Miura, T. Takiguchi and S. Okada, *Journal of the American Chemical Society*, 2003, **125**, 12971-12979.

63.   H. H. Chou and C. H. Cheng, *Advanced Materials*, 2010, **22**, 2468-2471.

64.   W. Holzer, A. Penzkofer and T. Tsuboi, *Chemical Physics*, 2005, **308**, 93-102.

65.   R. Abramovitch, G. C. Seng and A. Notation, *Canadian Journal of Chemistry*, 1960, **38**, 761-771.

66.   N. Miyaura and A. Suzuki, *Chemical Reviews*, 1995, **95**, 2457-2483.

67.   N. Miyaura, T. Yanagi and A. Suzuki, *Synthetic Communications*, 1981, **11**, 513-519.

68.   R. Chinchilla and C. Nájera, *Chemical Reviews*, 2007, **107**, 874-922.

69.   K. Sonogashira, *Journal of Organometallic Chemistry*, 2002, **653**, 46-49.

70.   A. Elangovan, Y.-H. Wang and T.-I. Ho, *Organic Letters*, 2003, **5**, 1841-1844.

71.   M. Bakherad, *Applied Organometallic Chemistry*, 2013, **27**, 125-140.

72.   R. Edkins, PG Thesis, Durham, 2011.

73.   K.-i. Yamashita, K.-i. Sato, M. Kawano and M. Fujita, *New Journal of Chemistry*, 2009, **33**, 264-270.

74.   M. Benstead, G. A. Rosser, A. Beeby, G. H. Mehl and R. W. Boyle, *Photochemical & Photobiological Sciences*, 2011, **10**, 992-999.

75.   F. H. Allen, O. Kennard, D. G. Watson, L. Brammer, A. G. Orpen and R. Taylor, *Journal of the Chemical Society, Perkin Transactions 2*, 1987, S1-S19.

76.   S. A. Denisov, Y. Cudré, P. Verwilst, G. Jonusauskas, M. Marín-Suárez, J. F. Fernández-Sánchez, E. Baranoff and N. D. McClenaghan, *Inorganic Chemistry*, 2014, **53**, 2677-2682.

77.   A. B. S. Rutter, *Unpublished PG Thesis*, 2007.

78.   D. Malacara, 2011.

79.   K. H. Kim, C. K. Moon, J. H. Lee, S. Y. Kim and J. J. Kim, *Advanced Materials*, 2014, **26**, 3844-3847.

80.   E. Baranoff, B. F. Curchod, J. Frey, R. Scopelliti, F. Kessler, I. Tavernelli, U. Rothlisberger, M. Grätzel and M. K. Nazeeruddin, *Inorganic chemistry*, 2011, **51**, 215-224.

81.   A. Roggan, O. Minet, C. Schröder and G. Müller, *Medical Optical Tomography: Functional Imaging and Monitoring*, 1993, 149-165.

82.   M. J. Frisch, G. W. Trucks, H. B. Schlegel, G. E. Scuseria, M. A. Robb, J. R. Cheeseman, G. Scalmani, V. Barone, B. Mennucci, G. A. Petersson, H. Nakatsuji, M. Caricato, X. Li, H. P. Hratchian, A. F. Izmaylov, J. Bloino, G. Zheng, J. L. Sonnenberg, M. Hada, M. Ehara, K. Toyota, R. Fukuda, J. Hasegawa, M. Ishida, T. Nakajima and O. K. Y. Honda, H. Nakai, T. Vreven, J. A. Montgomery, Jr., J. E. Peralta, F. Ogliaro, M. Bearpark, J. J. Heyd, E. Brothers, K. N. Kudin, V. N. Staroverov, R. Kobayashi, J. Normand, K. Raghavachari, A. Rendell, J. C. Burant, S. S. Iyengar, J. Tomasi, M. Cossi, N. Rega, J. M. Millam, M. Klene, J. E. Knox, J. B. Cross, V. Bakken, C. Adamo, J. Jaramillo, R. Gomperts, R. E. Stratmann, O. Yazyev, A. J. Austin, R. Cammi, C. Pomelli, J. W. Ochterski, R. L. Martin, K. Morokuma, V. G. Zakrzewski, G. A. Voth, P. Salvador, J. J. Dannenberg, S. Dapprich, A. D. Daniels,

Ö. Farkas, J. B. Foresman, J. V. Ortiz, J. Cioslowski, and D. J. Fox., Gaussian, Inc, Wallingford CT, Editon edn., 2009.

83.   A. D. Becke, *The Journal of Chemical Physics*, 1993, **98**, 5648-5652.

84.   P. J. Stephens, F. J. Devlin, C. F. Chabalowski and M. J. Frisch, *The Journal of Physical Chemistry*, 1994, **98**, 11623-11627.